

**( $p,d$ ) Reaction on  $N=Z$  Nuclei in the  $2s-1d$  Shell\***

R. L. KOZUB†

*Cyclotron Laboratory, Michigan State University, East Lansing, Michigan*

(Received 26 January 1968)

An investigation of the ( $p,d$ ) reaction on  $N=Z$  nuclei in the  $2s-1d$  shell has been made to obtain spectroscopic information and to study the  $l_n=2$   $J$ -dependence for the ( $p,d$ ) reaction. The experiments were performed with  $^{24}\text{Mg}$ ,  $^{28}\text{Si}$ ,  $^{32}\text{S}$ ,  $^{36}\text{Ar}$ , and  $^{40}\text{Ca}$  as target nuclei, and virtually all of the  $2s-1d$  shell hole strength was observed. Deuteron angular distributions for strongly excited levels in  $^{23}\text{Mg}$ ,  $^{27}\text{Si}$ ,  $^{31}\text{S}$ ,  $^{35}\text{Ar}$ , and  $^{39}\text{Ca}$  were measured for laboratory angles from  $10^\circ$  to  $155^\circ$ , and spectroscopic factors were obtained using distorted-wave Born-approximation (DWBA) calculations. The  $J$  dependence for the pickup of an  $l_n=2$  neutron appears mostly in the forward angles of the angular distributions and seems to follow systematic trends through the  $2s-1d$  shell, thus suggesting spin assignments for levels in  $^{31}\text{S}$ ,  $^{35}\text{Ar}$ , and  $^{39}\text{Ca}$ . Appreciable configuration mixing is found to exist in the ground-state wave functions of all the nuclei investigated. Of particular interest are the  $l_n=1$  levels excited in the  $^{24}\text{Mg}(p,d)^{23}\text{Mg}$  and  $^{28}\text{Si}(p,d)^{27}\text{Si}$  reactions, which could arise from the removal of either  $1p$ - or  $2p$ -shell neutrons. The ground states of  $^{36}\text{Ar}$  and  $^{40}\text{Ca}$  are observed to contain appreciable mixing with the  $f_{7/2}$  shell, and evidence exists for a small  $[2p]$ <sup>2</sup> admixture in the  $^{40}\text{Ca}$  ground state. The level orders of the residual nuclei and the DWBA spectroscopic factors are discussed in terms of the strong-coupling rotational model and Nilsson-model wave functions. Evidence for strong rotational band mixing is apparent in many cases.

**I. INTRODUCTION**

SINCE its original observation by Standing in 1954,<sup>1</sup> the ( $p,d$ ) reaction has been found to be a valuable tool for the experimental investigation of nuclear properties. This has proven to be particularly true at higher bombarding energies, where the direct-reaction theory is most successful. The widely used theory of direct-reaction processes is the distorted-wave Born approximation (DWBA)<sup>2</sup> and, to the extent that one can trust the DWBA calculations, the ( $p,d$ ) reaction provides a direct measure of the overlap of the target wave function with the wave functions of the excited states of the residual nucleus. Configuration admixtures in the target nucleus are thus easily detectable by this reaction.

In 1964 it was observed by Lee and Schiffer<sup>3</sup> that the angular distributions for  $l_n=1$  levels excited in the ( $d,p$ ) reaction on spin-zero targets showed a dependence on the total angular momentum of the final nuclear state. Similar effects have also been observed in the ( $p,d$ ) reaction,<sup>4-7</sup> where most of the previous investigations have been with nuclei in the  $1p$  and  $1f_{7/2}$  shells. However, relatively few ( $p,d$ ) experiments have been performed on the  $N=Z$  targets in the  $2s-1d$  shell. This probably reflects the very negative reaction  $Q$  values ( $-13$  to  $-15$  MeV) and the close level spacings in-

olved, which require both a high bombarding energy and good resolution in order to observe the level structure over a reasonable region of excitation in the residual nucleus.

The subject of this paper is an investigation of the ( $p,d$ ) reaction on  $^{24}\text{Mg}$ ,  $^{28}\text{Si}$ ,  $^{32}\text{S}$ ,  $^{36}\text{Ar}$ , and  $^{40}\text{Ca}$ . The primary objectives were to study the configuration mixing in the ground-state wave functions of the target nuclei and the  $l_n=2$   $J$ -dependence in the deuteron angular distributions. In addition, information concerning the level structures of the residual nuclei ( $^{23}\text{Mg}$ ,  $^{27}\text{Si}$ ,  $^{31}\text{S}$ ,  $^{35}\text{Ar}$ , and  $^{39}\text{Ca}$ ) was obtained. The bombarding energy of 33.6 MeV was low enough to be compatible with the use of commercially available, high-resolution semiconductor detectors; at the same time it was high enough to expose 10-12 MeV of excitation in the residual nuclei.

**II. EXPERIMENTAL METHODS**

The 33.6-MeV protons were obtained by accelerating negative hydrogen ions with the 64-in. Michigan State University sector-focusing cyclotron<sup>8</sup> and extracting a single turn with a 0.0001-in. aluminum stripper foil. Two quadrupole magnets and a  $20^\circ$  bending magnet were used to focus the beam into the 36-in. scattering chamber. The beam was collected in a Faraday cup at the rear of the scattering chamber, and the charge was summed by a current integrator with an error of less than 1%. Beam currents ranged from 1 to 100 nA, depending on the scattering angle. The energy of the proton beam from the cyclotron was measured by the kinematic crossover method<sup>9</sup> and checked by an independent range-energy calibration. The two methods were in agreement to within  $\sim 200$  keV.

<sup>8</sup> H. G. Blosser and A. I. Galonsky (unpublished).<sup>9</sup> B. M. Bardin and M. E. Rickey, *Rev. Sci. Instr.* **35**, 902 (1964).

\* Research supported by the National Science Foundation.

† Present address: Cyclotron Institute, Texas A &amp; M University, College Station, Tex.

<sup>1</sup> K. G. Standing, *Phys. Rev.* **94**, 731 (1954).<sup>2</sup> G. R. Satchler, *Nucl. Phys.* **55**, 1 (1964).<sup>3</sup> L. L. Lee, Jr., and J. P. Schiffer, *Phys. Rev. Letters* **12**, 108 (1964).<sup>4</sup> R. Sherr, E. Rost, and M. E. Rickey, *Phys. Rev. Letters* **12**, 420 (1964).<sup>5</sup> C. Glashauser and M. E. Rickey, *Phys. Rev.* **154**, 1033 (1967).<sup>6</sup> C. A. Whitten, Jr., E. Kashy, and J. P. Schiffer, *Nucl. Phys.* **86**, 307 (1966).<sup>7</sup> R. L. Kozub and E. Kashy, *Bull. Am. Phys. Soc.* **12**, 644 (1967).

The reaction products were observed with a  $dE/dx-E$  counter telescope consisting of a 279- $\mu$  silicon surface-barrier detector ( $\Delta E$ ) and a 3-mm lithium-drifted silicon counter ( $E$ ). This thickness for the  $\Delta E$  counter would stop only those deuterons having energy  $\lesssim 8$  MeV, which permitted the observation of 10–12 MeV of excitation in the nuclei studied. The telescope was mounted on a movable arm in the scattering chamber which could be positioned by remote control to an angular accuracy of  $\pm 0.5^\circ$ . The solid angle was defined by a tantalum collimator subtending an angle of  $\sim 1^\circ$ . For the gas targets used in the  $^{32}\text{S}(p, d)^{31}\text{S}$  and  $^{36}\text{Ar}(p, d)^{35}\text{Ar}$  experiments, an additional collimator was necessary to define the solid angle.

The deuteron pulses were electronically selected and sorted by a particle-identification circuit.<sup>10</sup> An over-all electronic noise width of 50 keV was obtained and the over-all deuteron energy resolution varied from 95 to 130 keV. The error in the absolute cross sections is estimated to be  $\pm 7\%$ , excluding the statistical error.

A detector consisting of CsI(Tl) crystal mounted on a photomultiplier tube was used as a monitor throughout the work. This same detector was used to obtain the  $^{26}\text{Mg}(p, p)^{26}\text{Mg}$  and  $^{36}\text{Ar}(p, p)^{36}\text{Ar}$  elastic scattering data with an over-all resolution of approximately 650 keV.

The ground-state  $(p, d)$  reaction  $Q$  values for the nuclei studied ranged from  $-14.95$  MeV for the  $^{28}\text{Si}(p, d)^{27}\text{Si}$  reaction to  $-12.86$  MeV for the  $^{32}\text{S}(p, d)^{31}\text{S}$  reaction. Since the  $Q$  values for the  $^{16}\text{O}(p, d)^{15}\text{O}$  and  $^{12}\text{C}(p, d)^{11}\text{C}$  reactions are in the same region ( $-13.44$  and  $-16.50$  MeV, respectively) and the  $^{15}\text{O}$  and  $^{11}\text{C}$  energy levels are well known,<sup>11</sup> deuteron spectra from  $^{16}\text{O}$  and  $^{12}\text{C}$  provided an excellent energy calibration.

The target used for the  $^{24}\text{Mg}(p, d)^{23}\text{Mg}$  experiment was a rolled foil of 1.07 mg/cm<sup>2</sup> thickness which was enriched to  $>99\%$   $^{24}\text{Mg}$ . A  $0.88 \pm 0.04$ -mg/cm<sup>2</sup> SiO

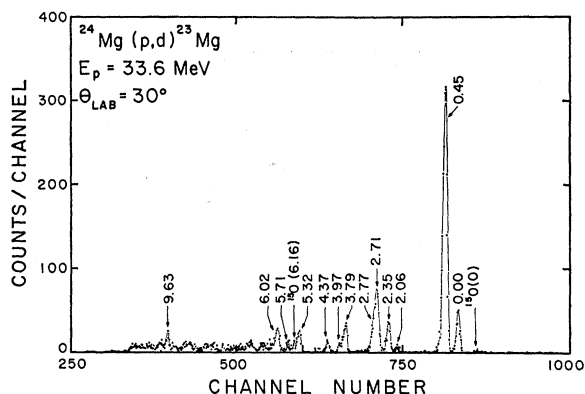


FIG. 1. Deuteron spectrum from  $^{24}\text{Mg}(p, d)^{23}\text{Mg}$  reaction at  $\theta_{\text{lab}} = 30^\circ$ , showing levels of  $^{23}\text{Mg}$ . A small oxygen contaminant is observed.

<sup>10</sup> F. S. Goulding, D. A. Landis, J. Cerny, and R. J. Pehl, Nucl. Instr. Methods **31**, 1 (1964).

<sup>11</sup> T. Lauritsen and F. Ajzenberg-Selove, *Energy Levels of Light Nuclei* (National Academy of Sciences-National Research Council, Washington, D. C., 1961).

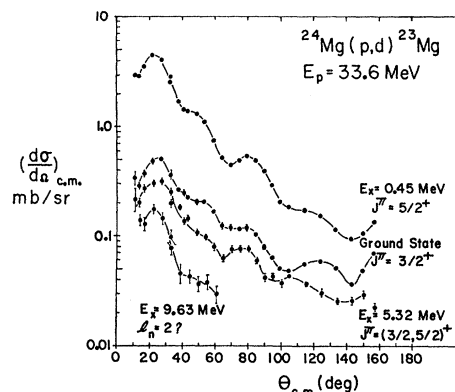


FIG. 2. Deuteron angular distributions corresponding to  $l_n = 2$  pickup in the  $^{24}\text{Mg}(p, d)^{23}\text{Mg}$  reaction. The error bars refer only to statistics and, where not shown, are smaller than the data points. The curves are drawn only to guide the eyes. The  $J$  dependence in the distributions for the ground and 0.45-MeV levels is generally opposite to that observed for most of the other  $s$ - $d$  shell nuclei studied.

target was fabricated by evaporating chemically pure SiO of natural isotopic abundance (92.2%  $^{28}\text{Si}$ ) to a 0.0001-in. nickel backing, and etching away a 2-cm<sup>2</sup> area of the nickel with  $\text{HNO}_3$ .

A gas target containing  $\text{H}_2\text{S}$  was used to study the  $^{32}\text{S}(p, d)^{31}\text{S}$  reaction. The gas cell consisted of a 5-in.-diam by 1-in.-high copper cylinder with 0.001-in. Kapton walls. The cell was filled to a pressure of 45 cm of Hg with natural  $\text{H}_2\text{S}$  (95.0%  $^{32}\text{S}$ ). A leakproof cell with Havar walls of 10 mg/cm<sup>2</sup> thickness was constructed for the purpose of making a permanent, isotopically enriched ( $>99\%$ )  $^{36}\text{Ar}$  gas target. A compound pressure gauge was mounted on the cell, which was filled with  $^{36}\text{Ar}$  to a pressure of  $45.1 \pm 1.0$  cm of Hg at  $25^\circ\text{C}$ .

Natural calcium foils (97.0%  $^{40}\text{Ca}$ ) were used in the study of the  $^{40}\text{Ca}(p, d)^{39}\text{Ca}$  reaction. These targets were made by evaporating calcium metal, and experimental data was obtained with foils of 1.10, 1.67, and 2.27 mg/cm<sup>2</sup> thickness.

### III. EXPERIMENTAL RESULTS

#### A. $^{24}\text{Mg}(p, d)^{23}\text{Mg}$

A typical deuteron spectrum from the  $(p, d)$  reaction on the  $^{24}\text{Mg}$  target (Fig. 1) shows that several levels of  $^{23}\text{Mg}$  are strongly excited. The excitation of  $^{15}\text{O}$  levels at 0.00 and 6.16 MeV indicates a slight oxidation of the target. An over-all deuteron energy resolution of 115–120 keV was obtained. This was insufficient to resolve the 2.71- and 2.77-MeV levels of  $^{23}\text{Mg}$ ; a similar situation exists for the 3.79- and 3.86-MeV levels. Consequently, the 2.71- and 3.79-MeV levels were analyzed by assuming that their peak shapes were the same as the well-resolved 0.45-MeV level.

Deuteron angular distributions for 10 of the excited levels were measured for laboratory angles from  $10^\circ$  to

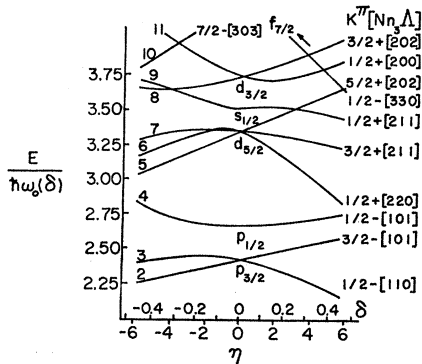


FIG. 3. Nilsson diagram of single-particle levels in a deformed well (Ref. 14). Each level can hold at most two protons and two neutrons; the first  $K = \frac{1}{2}$  ( $2s_{1/2}$ ) level is not shown. (From Ref. 15.)

155°. The distributions for levels of  $^{23}\text{Mg}$  at 0.00, 0.45, and 5.32 MeV shown in Fig. 2 indicate a neutron pickup from the  $1d$  shell ( $l_n = 2$ ) and are consistent with spin and parity assignments  $J^\pi = \frac{3}{2}^+$ ,  $\frac{5}{2}^+$ , and  $(\frac{3}{2}, \frac{5}{2})^+$ , respectively. The angular distribution for a level at 9.63 MeV is also shown, and corresponds to an  $l_n$  of either 1 or 2. The position of the forward maximum seems to favor slightly the  $l_n = 2$  assignment, although the statistical errors are quite large. The assignments for the 0.00- and 0.45-MeV levels correspond to well-known mirror levels in  $^{23}\text{Na}$ , and have been confirmed recently by  $^{24}\text{Mg}-(^3\text{He}, \alpha)^{23}\text{Mg}$  experiments.<sup>12,13</sup> They are interpreted<sup>13</sup> as corresponding to members of a rotational band based on a  $K = \frac{3}{2}$  hole in Nilsson orbit 7<sup>14</sup> (See Fig. 3). This seems reasonable since the nuclear deformations in this mass region are assumed to be prolate ( $\delta > 0$ ).<sup>15</sup> The third member of this band should be the  $\frac{7}{2}^+$  level at 2.06 MeV. The angular distribution for this level (Fig. 4) is relatively isotropic, indicating that a compound-nucleus reaction mechanism is involved rather than a direct

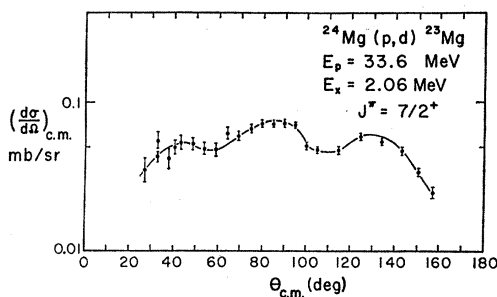


FIG. 4. Deuteron angular distribution for the 2.06-MeV level of  $^{23}\text{Mg}$  from the  $^{24}\text{Mg}(p,d)^{23}\text{Mg}$  reaction.

<sup>12</sup> J. M. Joyce, R. W. Zurmühle, and C. M. Fou, *Bull. Am. Phys. Soc.* **11**, 908 (1966).

<sup>13</sup> J. Dubois and L. G. Earwaker, *Bull. Am. Phys. Soc.* **11**, 908 (1966).

<sup>14</sup> S. G. Nilsson, *Kgl. Danske Videnskab. Selskab, Mat. Fys. Medd.* **29**, No. 16 (1955).

<sup>15</sup> M. A. Preston, *Physics of the Nucleus* (Addison-Wesley Publishing Co., Inc., Reading, Mass., 1962).

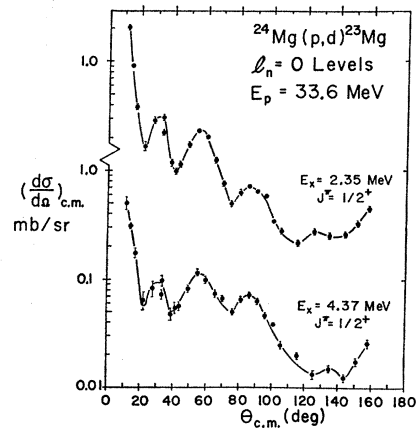


FIG. 5. Deuteron angular distributions corresponding to  $l_n = 0$  pickup in the  $^{24}\text{Mg}(p,d)^{23}\text{Mg}$  reaction.

process, which would have indicated some admixture with the  $g_{7/2}$  shell in the target state.

The levels at 2.35 and 4.37 MeV are excited by an  $l_n = 0$  pickup (Fig. 5) and therefore have  $J^\pi = \frac{1}{2}^+$ . Levels in  $^{23}\text{Na}$  with the same  $J$  have been observed at similar excitation energies.<sup>16</sup> The 2.35-MeV level is assumed to be excited mainly by a pickup from Nilsson orbit 6.<sup>13</sup> On the basis of the Nilsson model (Fig. 3), there should be just one  $\frac{1}{2}^+$  level excited in  $^{23}\text{Mg}$  by a direct pickup. The excitation of both the 2.35- and 4.37-MeV levels is therefore evidence for configuration mixing between Nilsson orbits.

The angular distributions obtained for the 2.71-, 3.79-, and 6.02-MeV levels of  $^{23}\text{Mg}$  have shapes corresponding to  $l_n = 1$  pickup, which indicates that these levels have negative parity with  $J = \frac{1}{2}$  or  $\frac{3}{2}$  (Fig. 6). The spin and parity of the 2.64-MeV level of  $^{23}\text{Na}$ , which could be the mirror to the 2.71-MeV level of  $^{23}\text{Mg}$ , has

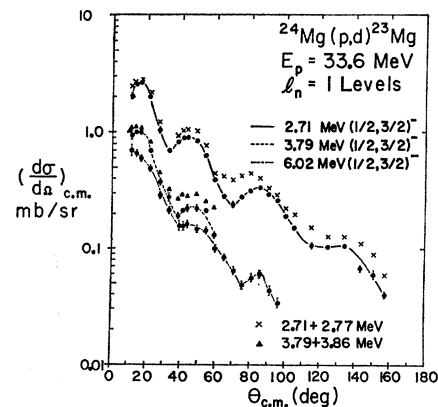
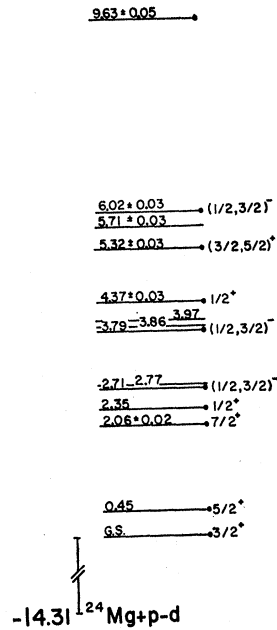


FIG. 6. Deuteron angular distributions corresponding to  $l_n = 1$  pickup in the  $^{24}\text{Mg}(p,d)^{23}\text{Mg}$  reaction. The distributions for the composite peaks at 2.7 and 3.8 MeV are also shown.

<sup>16</sup> O. Hansen, E. Koltay, N. Lund, and B. S. Madsen, *Nucl. Phys.* **51**, 307 (1964).

FIG. 7.  $^{23}\text{Mg}$  levels observed in the  $^{24}\text{Mg}(p, d)^{23}\text{Mg}$  reaction. The heavy dots indicate levels for which angular distributions were measured.



been previously reported as  $\frac{1}{2}^+$ .<sup>17</sup> DuBois and Earwaker,<sup>18</sup> who have recently studied the  $^{24}\text{Mg}(^3\text{He}, \alpha)^{23}\text{Mg}$  reaction, have confirmed the assignments given here for the 3.79- and 6.02-MeV levels. However, they conclude that the excitation of the 2.77-MeV level is due to an  $l_n=1$  pickup, while the level at 2.71 MeV is possibly excited by an  $l_n=3$  transfer. The energies measured for these two levels in the present work are estimated to be in error by about  $\pm 20$  keV, and it appears from the deuteron spectrum (Fig. 1) that the most strongly excited level in the doublet corresponds to the lowest excitation energy. It was this portion of the composite peak that was analyzed by the method

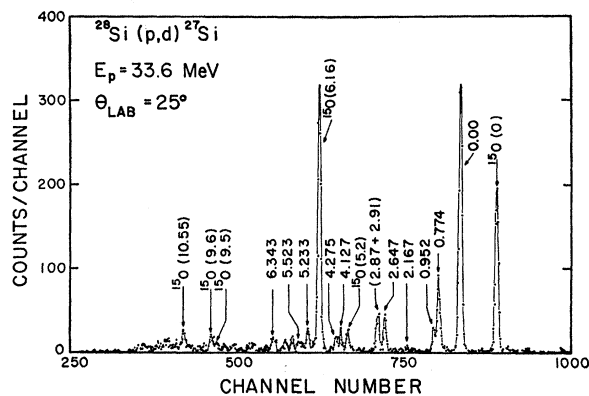


FIG. 8. Deuteron spectrum from the  $^{28}\text{Si}(p, d)^{27}\text{Si}$  reaction at  $\theta_{\text{lab}} = 25^\circ$ . A SiO target was used, and levels of  $^{16}\text{O}$  and  $^{27}\text{Si}$  are indicated.

<sup>17</sup> D. W. Braben, L. L. Green, and J. C. Willmott, Nucl. Phys. 32, 584 (1962).

<sup>18</sup> J. Dubois and L. G. Earwaker, Phys. Rev. 160, 925 (1967).

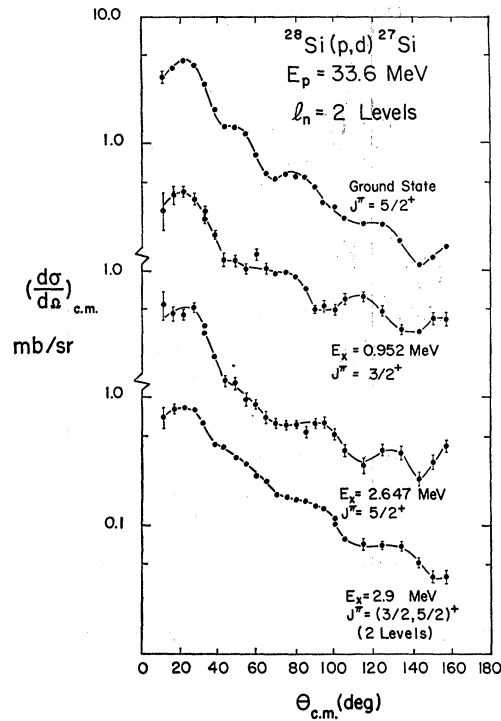


FIG. 9. Deuteron angular distributions corresponding to  $l_n=2$  pickup in the  $^{28}\text{Si}(p, d)^{27}\text{Si}$  reaction. Very little  $J$  dependence is observed in the distributions for the ground and 0.952-MeV levels.

discussed earlier to obtain the angular distribution shown in Fig. 6.

A summary of the results obtained from the  $^{24}\text{Mg}(p, d)^{23}\text{Mg}$  reaction is given in the level diagram of Fig. 7. In addition to the levels shown here, several others have been observed recently in  $^{24}\text{Mg}(^3\text{He}, \alpha)^{23}\text{Mg}$  experiments.<sup>12,13,19</sup> The energies for four of the levels are

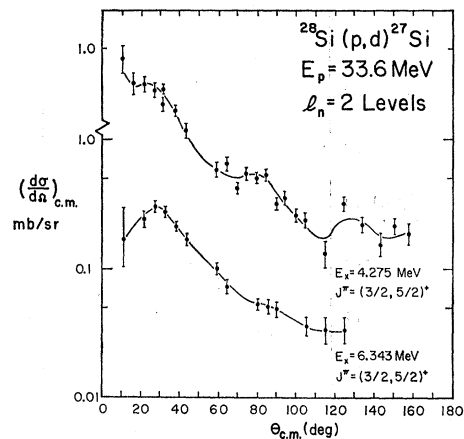


FIG. 10. Deuteron angular distributions corresponding to  $l_n=2$  pickup in the  $^{28}\text{Si}(p, d)^{27}\text{Si}$  reaction.

<sup>19</sup> H. J. Hay and D. C. Keen, Nucl. Phys. A98, 330 (1967).

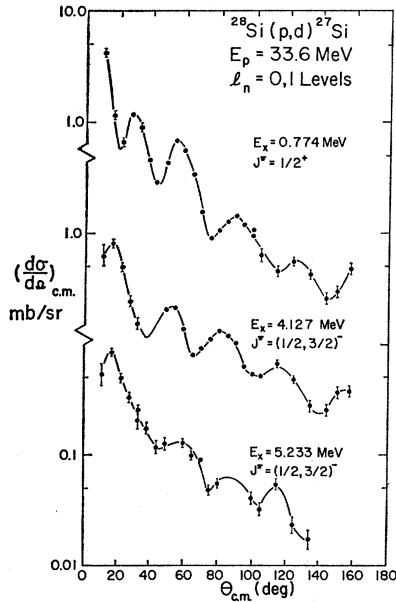


FIG. 11. Deuteron angular distributions corresponding to  $l_n=0$  and 1 pickup in the  $^{28}\text{Si}(p,d)^{27}\text{Si}$  reaction.

in agreement with those found by Ref. 19 at 4.362, 5.286, 5.7 (doublet), and 5.986 MeV.

$J$  dependence for the  $^{24}\text{Mg}(p,d)^{23}\text{Mg}$  reaction is observed in the angular distributions for the ground ( $\frac{3}{2}^+$ ) and 0.45-MeV ( $\frac{5}{2}^+$ ) levels of  $^{23}\text{Mg}$  (Fig. 2). The  $\frac{5}{2}^+$  distribution has a steeper over-all slope versus angle than the  $\frac{3}{2}^+$  distribution, while the forward maximum for  $J=\frac{5}{2}$  seems to occur at a slightly smaller angle than for  $J=\frac{3}{2}$ . Although the  $J$  dependence here seems relatively weak, the effects are generally opposite to those observed for most of the other nuclei investigated in this study.

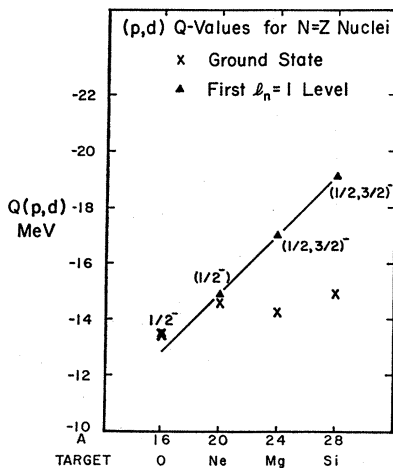


FIG. 12. Plot of  $(p,d)$  reaction  $Q$  values to the first  $l_n=1$  level in  $N=Z$  nuclei versus target mass number. A straight line is drawn for comparison.

B.  $^{28}\text{Si}(p,d)^{27}\text{Si}$

A typical deuteron spectrum from the  $(p,d)$  reaction on the SiO target is shown in Fig. 8. Several excited levels of  $^{27}\text{Si}$  and  $^{15}\text{O}$  were observed with an over-all energy resolution of 95–100 keV. The differential cross sections for the  $^{27}\text{Si}$  levels were obtained at angles where, because of kinematic effects, they were unresolved from  $^{15}\text{O}$  levels, by interpolating both the oxygen and silicon angular distributions.

1. Positive Parity Levels

Six deuteron groups from the  $^{28}\text{Si}(p,d)^{27}\text{Si}$  reaction are observed to arise mainly from an  $l_n=2$  neutron pickup (Figs. 9 and 10). Spin and parity assignments of  $\frac{3}{2}^+$ ,  $\frac{5}{2}^+$ , and  $\frac{7}{2}^+$  for excitation energies 0.00, 0.952, and 2.647 MeV, respectively, are obtained from corresponding levels of known spin and parity in the  $^{27}\text{Al}$  mirror nucleus.<sup>20</sup> The 2.90-MeV peak is known to consist of two levels which are separated by about 40 keV, one of which has been assigned  $J=\frac{3}{2}^+$ .<sup>20</sup> Since the full width at half-maximum (FWHM) of this group in the spectrum (Fig. 8) is about 40 keV larger than that for the other levels, it appears that both levels may be strongly excited. Therefore, since the sum of their angular distributions retains the  $l_n=2$  shape, the assignment  $J^\pi = (\frac{3}{2}, \frac{5}{2})^+$  may be reasonable for both levels, unless one of them is not excited by a direct process. A recent  $^{28}\text{Si}(d,^3\text{He})^{27}\text{Al}$  experiment, where the mirror of this doublet was resolved, has indicated that the angular distribution for one of the levels is relatively isotropic.<sup>21</sup>

The angular distribution for the 4.275-MeV level (Fig. 10) indicates some admixtures from other unresolved levels having  $l_n \neq 2$ , but the main contribution appears to be from the  $1d$  shell, resulting in a  $(\frac{3}{2}, \frac{5}{2})^+$  assignment for this level and the level at 6.343-MeV

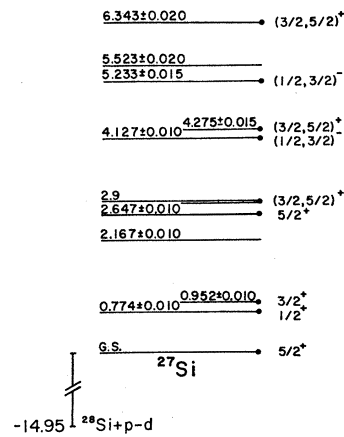


FIG. 13.  $^{27}\text{Si}$  levels observed in the  $^{28}\text{Si}(p,d)^{27}\text{Si}$  reaction.

<sup>20</sup> P. M. Endt and C. Van der Leun, Nucl. Phys. 34, 1 (1962).

<sup>21</sup> H. E. Gove et al., Bull. Am. Phys. Soc. 12, 665 (1967); H. E. Gove (private communication).

excitation. This assignment has also been obtained for a level in  $^{27}\text{Al}$  at 4.403 MeV from the  $^{28}\text{Si}(d,^3\text{He})^{27}\text{Al}$  reaction.<sup>22</sup>

The excitation of the 0.77-MeV level is evidence for a  $2s_{1/2}$  admixture in the  $^{28}\text{Si}$  ground state. The  $l_n=0$  angular distribution for this level is shown in Fig. 11, and the  $\frac{1}{2}^+$  assignment is consistent with that for the first excited state of  $^{27}\text{Al}$ .<sup>20</sup>

The fact that the  $^{27}\text{Si}$  ground state has  $J^\pi = \frac{5}{2}^+$  would suggest a spherical or prolate shape ( $\delta \geq 0$ ) on the basis of the Nilsson model (Fig. 3), but the existence of the  $\frac{1}{2}^+$  level at low excitation energy (0.774 MeV) suggests a pickup from Nilsson orbit 6 with an oblate deformation ( $\delta < 0$ ). Also, the 0.952-MeV  $\frac{3}{2}^+$  level could be excited by removing a neutron from orbit 7 with either a positive or a negative  $\delta$ . It is thus difficult to interpret the ground state of  $^{28}\text{Si}$  in terms of a simple Nilsson model.

Little  $J$  dependence is observed in the  $^{28}\text{Si}(p, d)^{27}\text{Si}$  reaction. The angular distributions for the ground ( $\frac{5}{2}^+$ ) and 0.952-MeV levels ( $\frac{3}{2}^+$ ) (Fig. 9) are similar in shape, although there seems to be a flattening of the cross section for the  $\frac{3}{2}^+$  level for  $\theta_{c.m.} \gtrsim 60^\circ$ . The angle at which the forward maximum appears in the  $\frac{3}{2}^+$  distribution is about the same, or slightly smaller, than for  $J = \frac{5}{2}$ .

## 2. Negative Parity Levels

The angular distributions for two  $l_n=1$  levels of  $^{27}\text{Si}$  at 4.127- and 5.233-MeV excitation are also shown in Fig. 11. The corresponding levels in the mirror nucleus have been observed by Wildenthal and Newman in the  $^{28}\text{Si}(d,^3\text{He})^{27}\text{Al}$  proton pickup reaction.<sup>22</sup> The predictions of Hartree-Fock calculations<sup>23</sup> and the conclusions of proton knockout experiments<sup>24,25</sup> indicate a separation energy difference between the  $1p$  and  $2s-1d$  shells of 10 to 20 MeV in this mass region. Because of their low

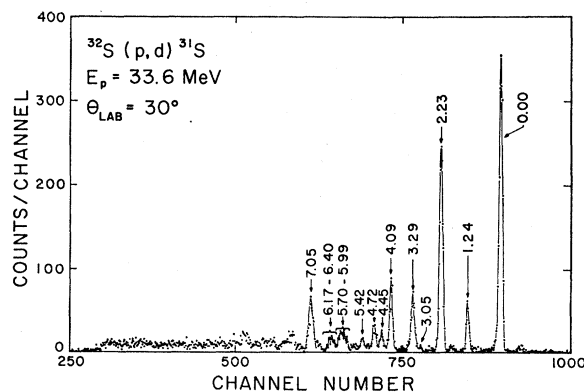


FIG. 14. Deuteron spectrum from the  $^{32}\text{S}(p, d)^{31}\text{S}$  reaction at  $\theta_{\text{lab}} = 30^\circ$ , showing levels of  $^{31}\text{S}$ . No strongly excited levels are observed at excitation energies greater than 7.05 MeV in  $^{31}\text{S}$ .

<sup>22</sup> B. H. Wildenthal and E. Newman, Phys. Rev. **167**, 1027 (1968).

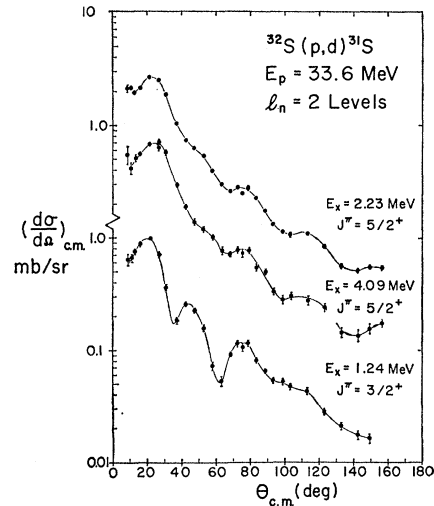


FIG. 15. Deuteron angular distributions corresponding to  $l_n=2$  pickup in the  $^{32}\text{S}(p, d)^{31}\text{S}$  reaction. The pronounced  $J$  dependence is similar to that observed by Ref. 5.

excitation energy these levels might be thought of as being excited mainly by a pickup from the  $2p$  shell. In Fig. 12 the  $(p, d)$  reaction  $Q$  values to the  $l_n=1$  levels of lowest excitation are plotted for the  $N=Z$ , even-even nuclei for  $A=16-28$  (Ref. 11 and this paper). Since the transition to the  $^{16}\text{O}$  ground state is due to a pickup from the  $1p_{1/2}$  shell, it seems reasonable, from the ob-

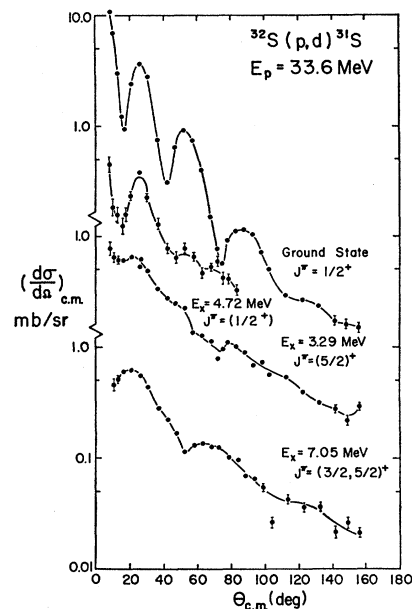


FIG. 16. Deuteron angular distributions corresponding to  $l_n=0$  and 2 pickup in the  $^{32}\text{S}(p, d)^{31}\text{S}$  reaction.

<sup>23</sup> K. T. R. Davies, S. J. Kreiger, and M. Baranger, Nucl. Phys. **84**, 545 (1966).

<sup>24</sup> M. Riou, Rev. Mod. Phys. **37**, 375 (1965).

<sup>25</sup> Gerhard Jacob and Th. A. J. Maris, Rev. Mod. Phys. **38**, 121 (1966).

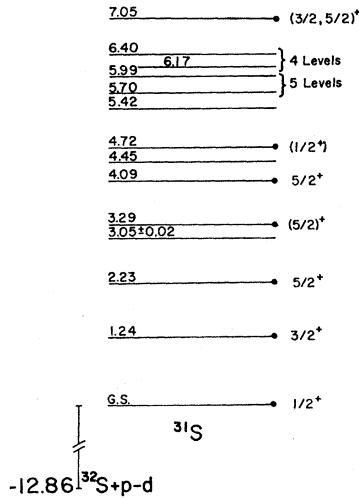


FIG. 17.  $^{31}\text{S}$  levels observed in the  $^{32}\text{S}(p,d)^{31}\text{S}$  reaction. The level energies for all but the 3.05-MeV level are in agreement with those measured by Ref. 26.

served trend in the neutron separation energy, that the  $l_n=1$  levels in the other nuclei are also excited by a  $1p$  pickup. The strengths of these excitations are of little help in resolving this ambiguity, since a DWBA calculation predicts a much lower spectroscopic factor for a  $2p$  pickup than for a  $1p$  pickup. Considering the plot in Fig. 12, however, one can conclude that the evidence for  $1p$  hole-state assignments for these levels is at least as strong as for an origin due to a  $2p$  admixture.

The excitation energies, spins and parities of the levels excited in the  $^{28}\text{Si}(p,d)^{27}\text{Si}$  reaction are shown in Fig. 13. The energy measurements for the first six excited levels are in agreement with Ref. 20 to within the experimental error. Due to the constant presence of well-known  $^{15}\text{O}$  levels in the spectrum, energy measurements with  $\pm 10$  keV error were possible in many cases.

### C. $^{32}\text{S}(p,d)^{31}\text{S}$

Figure 14 shows a deuteron spectrum from the  $(p,d)$  reaction on the  $\text{H}_2\text{S}$  gas target at a laboratory angle of

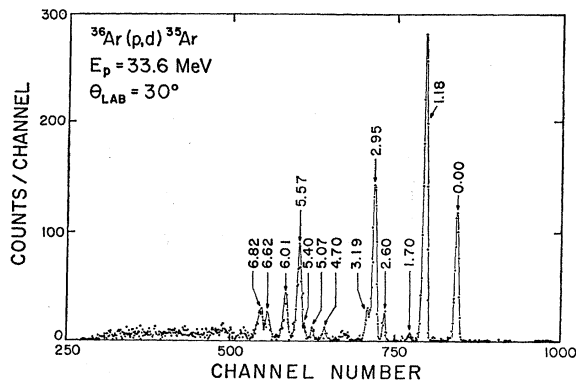


FIG. 18. Deuteron spectrum from the  $^{36}\text{Ar}(p,d)^{35}\text{Ar}$  reaction at  $\theta_{\text{lab}}=30^\circ$ , showing levels of  $^{35}\text{Ar}$ . It is apparent that most of the  $2s-1d$  shell hole strength is observed.

$30^\circ$ . The over-all resolution is about 120 keV. Many of the 39 levels observed in a  $^{32}\text{S}(^3\text{He},\alpha)^{31}\text{S}$  experiment<sup>26</sup> are confirmed, in addition to a very weak level at  $E_x = 3.05 \pm 0.02$  MeV which had been observed earlier.<sup>27,28</sup> No strongly excited  $^{31}\text{S}$  levels are observed for  $E_x > 7.05$  MeV.

The deuteron angular distributions from levels of  $^{31}\text{S}$  at 1.24-, 2.23-, and 4.09-MeV excitation energies are shown in Fig. 15. All of these distributions correspond to an  $l_n=2$  neutron pickup, and the respective assignments  $\frac{3}{2}^+$ ,  $\frac{5}{2}^+$ , and  $\frac{5}{2}^+$  are consistent with those for corresponding levels in the mirror nucleus  $^{31}\text{P}$ . Angular distributions were also measured for the 0.00-, 3.29-, 4.72-, and 7.05-MeV levels and are shown in Fig. 16. The ground state corresponds to an  $l_n=0$  pickup and has the expected spin and parity of  $\frac{1}{2}^+$ . The distribution for the 4.72-MeV level probably also corresponds to an  $l_n=0$  pickup. The 3.29-MeV level appears to be excited mainly by an  $l_n=2$  pickup, although the angular distribution indicates the presence of other admixtures. Ajzenberg-Selove and Wiza<sup>26</sup> have reported a level at  $3.359 \pm 0.015$  MeV, which would be unresolved here. A  $(\frac{5}{2})^+$  assignment would be consistent with the assignment for a mirror level in  $^{31}\text{P}$  at the same energy. The distribution for the 7.05-MeV level also corresponds to an  $l_n=2$  pickup, indicating that  $J^\pi = (\frac{3}{2}, \frac{5}{2})^+$  for this level.

The first three levels of  $^{31}\text{S}$  are the 0.00( $\frac{1}{2}^+$ ), 1.24( $\frac{3}{2}^+$ ), and 2.23 MeV ( $\frac{5}{2}^+$ ) levels, whose spins and parities are

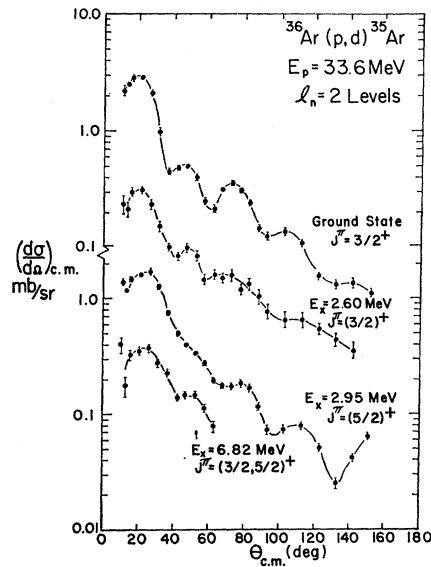


FIG. 19. Deuteron angular distributions corresponding to  $l_n=2$  pickup in the  $^{36}\text{Ar}(p,d)^{35}\text{Ar}$  reaction. The  $J$  dependence in the distributions for the ground and 2.95-MeV levels is similar to that observed in the  $^{32}\text{S}(p,d)^{31}\text{S}$  reaction.

<sup>26</sup> F. Ajzenberg-Selove and J. L. Wiza, Phys. Rev. 143, 853 (1966).

<sup>27</sup> J. J. Wesolowski, J. D. Anderson, L. F. Hansen, C. Wong, and J. W. McClure, Nucl. Phys. 71, 586 (1965).

<sup>28</sup> J. W. Nelson, E. B. Carter, G. E. Mitchell, and R. H. Davis, Phys. Rev. 129, 1723 (1963).

consistent with a rotational band based on a neutron hole in Nilsson orbit 9 (Fig. 3), if the deformation is such that the decoupling parameter for  $K = \frac{1}{2}$  does not affect the level order. However, the only sizable admixture with higher shells is with the  $d_{3/2}$  shell, which results in the strong excitation of the 1.24-MeV level.

Figure 17 shows the  $^{31}\text{S}$  levels excited in this reaction. The energy measurements are in agreement with the results of Ref. 26, with an experimental error of about  $\pm 20$  keV for each level.

The  $J^\pi = \frac{3}{2}^+$  and  $\frac{5}{2}^+$  angular distributions shown in Fig. 15 exhibit a striking example of  $J$  dependence in the  $1d$  shell, similar to that observed in the  $(p, d)$  reaction with 28-MeV protons.<sup>5</sup> The forward maximum of the 1.24-MeV level ( $\frac{3}{2}^+$ ) in  $^{31}\text{S}$  occurs at a smaller angle than the distributions for either the 2.23- or 4.09-MeV levels (both  $\frac{5}{2}^+$ ), and drops off much more rapidly to the first minimum. The oscillatory structure is much more pronounced for  $J = \frac{3}{2}^+$ ; in fact, the second maximum ( $\theta_{c.m.} \approx 45^\circ$ ) is barely noticeable in the angular distributions for the  $\frac{5}{2}^+$  levels. It is evident that for the 4.09-MeV level a spin and parity of  $J^\pi = \frac{5}{2}^+$  could have been assigned on the basis of  $J$  dependence alone.

#### D. $^{36}\text{Ar}(p, d)^{35}\text{Ar}$

Thirteen deuteron groups, corresponding to levels in  $^{35}\text{Ar}$ , were observed in the  $^{36}\text{Ar}(p, d)^{35}\text{Ar}$  reaction. A typical spectrum is shown in Fig. 18, where the over-all resolution is about 130 keV.

Angular distributions were measured for 10 levels of  $^{35}\text{Ar}$  and are shown in Figs. 19–21. The  $l_n = 2$  distributions for levels at 0.00-, 2.60-, 2.95-, and 6.82-MeV excitation (Fig. 19) show that they are excited by neutron pickup from the  $d_{3/2}$  and  $d_{5/2}$  shells. The spin assignments for the 2.60( $\frac{3}{2}^+$ ) and 2.95-MeV ( $\frac{5}{2}^+$ ) levels are made on the basis of the observed  $J$  dependence discussed below. The ground-state assignment of  $\frac{3}{2}^+$  corresponds to the spin and parity of the  $^{35}\text{Cl}$  mirror

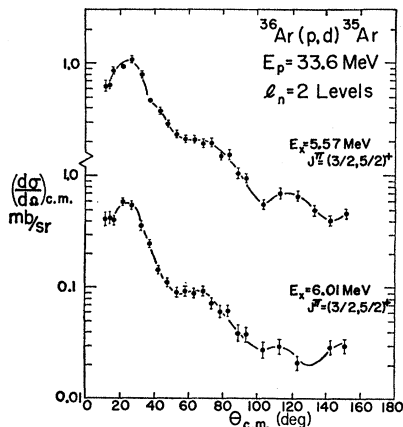


Fig. 20. Deuteron angular distributions corresponding to  $l_n = 2$  pickup in the  $^{36}\text{Ar}(p, d)^{35}\text{Ar}$  reaction.

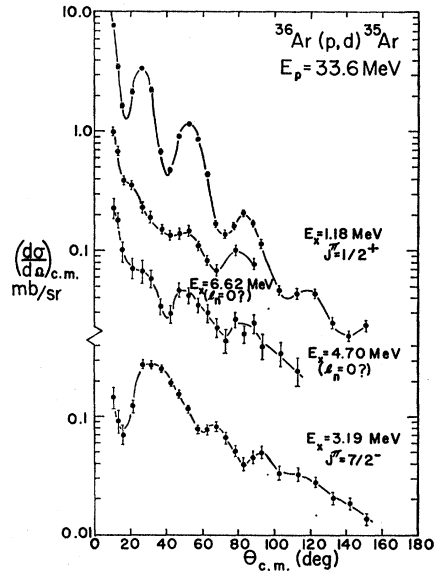


Fig. 21. Deuteron angular distributions from the  $^{36}\text{Ar}(p, d)^{35}\text{Ar}$  reaction. The excitation of the  $l_n = 3$  level at 3.19 MeV is evidence for appreciable configuration mixing with the  $f_{7/2}$  shell in the  $^{36}\text{Ar}$  ground state.

nucleus.<sup>20</sup> The spin of the 6.82-MeV level is uncertain but must be either  $\frac{3}{2}^+$  or  $\frac{5}{2}^+$ . The distributions for the 5.57- and 6.01-MeV levels also correspond to an  $l_n = 2$  pickup (Fig. 20) and are therefore assigned  $J^\pi = (\frac{3}{2}, \frac{5}{2})^+$ .

The angular distributions for the 1.18-, 3.19-, 4.70-, and 6.62-MeV levels of  $^{35}\text{Ar}$  are shown in Fig. 21. The first of these corresponds to an  $l_n = 0$  pickup and has  $J = \frac{1}{2}^+$ . The distribution for the 3.19-MeV level peaks at  $\theta_{c.m.} \approx 30^\circ$ , which indicates that this level is excited by the pickup of an  $l_n = 3$  neutron and corresponds to configuration mixing with the  $1f$  shell in the  $^{36}\text{Ar}$  ground state. The level is assigned  $J^\pi = \frac{7}{2}^-$  since it is most prob-

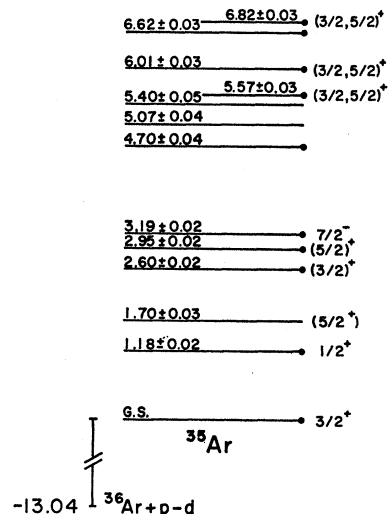


Fig. 22.  $^{35}\text{Ar}$  levels observed in the  $^{36}\text{Ar}(p, d)^{35}\text{Ar}$  reaction.

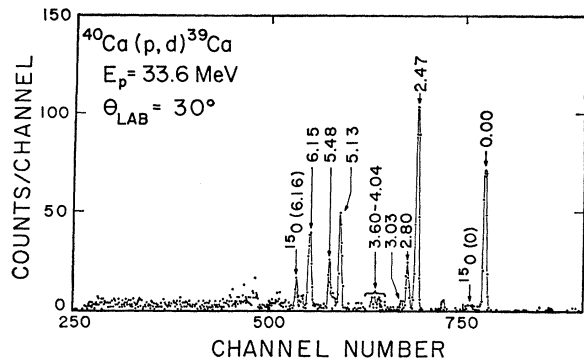


FIG. 23. Deuteron spectrum from the  $^{40}\text{Ca}(p,d)^{39}\text{Ca}$  reaction at  $\theta_{\text{lab}} = 30^\circ$ , showing levels of  $^{39}\text{Ca}$ . It is apparent that most of the  $2s-1d$  shell hole strength is observed. A small oxygen contaminant is also indicated.

able from a shell-model standpoint, and the mirror level in  $^{35}\text{Cl}$  is believed to have the same assignment.<sup>20</sup>

The assignments of the  $^{35}\text{Ar}$  levels at 0.00, 1.18, 1.70, 2.60, and 2.95 MeV as  $\frac{3}{2}^+$ ,  $\frac{1}{2}^+$ ,  $(\frac{5}{2}^+)$ ,  $\frac{3}{2}^+$ , and  $(\frac{5}{2}^+)$ , respectively, gives a level order consistent with that of rotational bands based on Nilsson orbits 8 (first and third levels) and 9 (second, fourth, and fifth levels) if the deformation is oblate and no inversions occur in the  $K = \frac{1}{2}[211]$  band. The assignment for the 1.70-MeV level as  $(\frac{5}{2}^+)$  is assumed from the mirror level in  $^{35}\text{Cl}$ .<sup>20</sup>

The diagram in Fig. 22 summarizes the information obtained about the level structure of  $^{35}\text{Ar}$  from the  $(p,d)$  reaction. The energies of the low-lying levels correspond closely to levels in the  $^{35}\text{Cl}$  mirror nucleus.<sup>20</sup>

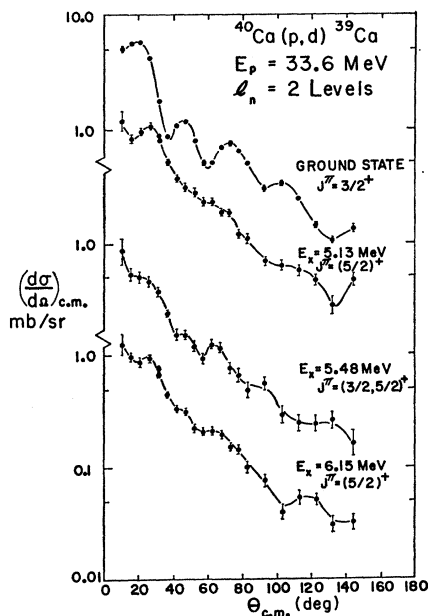


FIG. 24. Deuteron angular distributions corresponding to  $l_n = 2$  pickup in the  $^{40}\text{Ca}(p,d)^{39}\text{Ca}$  reaction. The  $J$  dependence in the distributions for the ground and 5.13-MeV levels is similar to that observed in the  $(p,d)$  reaction on  $^{36}\text{Ar}$  and  $^{32}\text{S}$ .

The  $J$  dependence observed in the  $^{36}\text{Ar}(p,d)^{35}\text{Ar}$  reaction for  $\frac{3}{2}^+$  and  $\frac{5}{2}^+$  levels (Fig. 19) is very similar to that for the  $^{32}\text{S}(p,d)^{31}\text{S}$  reaction. The angular distributions for the 2.23- and 4.09-MeV levels of  $^{31}\text{S}$  (Fig. 15) and the 2.95-MeV level of  $^{35}\text{Ar}$  are practically identical in shape for  $\theta_{\text{c.m.}} \lesssim 90^\circ$ . Since both of the  $^{31}\text{S}$  levels have  $J = \frac{5}{2}^+$ , the 2.95-MeV level of  $^{35}\text{Ar}$  is assigned  $J^\pi = (\frac{5}{2}^+)$ . The distributions for the ground and 2.60-MeV levels in  $^{35}\text{Ar}$  are similar to the distribution for the  $^{31}\text{S}$  1.24-MeV level ( $\frac{3}{2}^+$ ), although the oscillatory structure is not quite so pronounced. The existence of the  $45^\circ$  maximum and the relatively small angle for the forward maximum in the distribution for the 2.60-MeV level favors the assignment of  $J^\pi = (\frac{3}{2}^+)$ .

### E. $^{40}\text{Ca}(p,d)^{39}\text{Ca}$

The deuteron spectrum shown in Fig. 23 is similar to those obtained from the  $^{40}\text{Ca}(p,d)^{39}\text{Ca}$  reaction by Glashauser *et al.*<sup>29</sup> with 27.3-MeV protons. A natural calcium foil of 1.10 mg/cm<sup>2</sup> was used and a resolution of 100 keV was obtained; the normalization was checked with 1.67- and 2.27-mg/cm<sup>2</sup> foils. A small oxygen contaminant on the target is indicated by the presence of the  $^{15}\text{O}$  ground and 6.16-MeV levels in the spectrum. About 12 MeV of excitation in  $^{39}\text{Ca}$  is observed, and no appreciable strength appears beyond the 6.15-MeV level.

The angular distributions for the 0.00-, 5.13-, 5.48-, and 6.15-MeV levels shown in Fig. 24 all correspond to

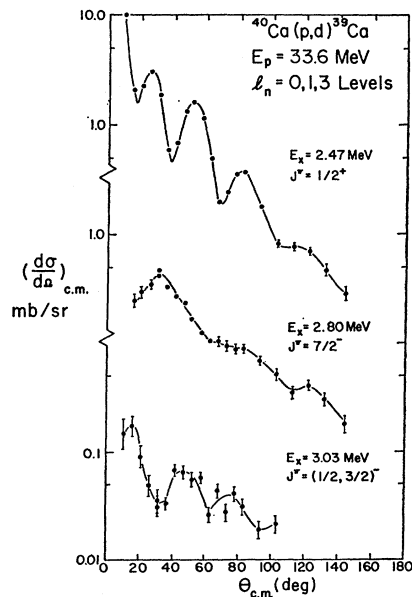


FIG. 25. Deuteron angular distributions from the  $^{40}\text{Ca}(p,d)^{39}\text{Ca}$  reaction. The excitation of the 2.80- ( $l_n = 3$ ) and 3.03-MeV ( $l_n = 1$ ) levels correspond to configuration mixing in the  $^{40}\text{Ca}$  ground state with the  $1f_{7/2}$  and  $2p_{1/2}$  shells, respectively.

<sup>29</sup> C. Glashauser, M. Kondo, M. E. Rickey, and E. Rost, Phys. Letters 14, 113 (1965).

an  $l_n=2$  pickup. The ground state has  $J^\pi = \frac{3}{2}^+$ , which corresponds to the spin and parity of the mirror nucleus  $^{39}\text{K}$ . The peak differential cross section obtained at 33.6-MeV bombarding energy was  $5.6 \pm 0.4$  mb/sr. Glashauser *et al.*<sup>29</sup> obtained a value of  $\sim 3$  mb/sr at 27.3-MeV bombarding energy, while Cavanagh *et al.*<sup>30</sup> measured  $\sim 4.5$  mb/sr for the peak cross section with 30-MeV protons. This indicates that differential cross section is quite sensitive to the bombarding energy.

The 5.13-MeV level is assigned  $J^\pi = (\frac{5}{2})^+$  on the basis of the  $J$  dependence observed in the angular distributions (see below). Although the angular distribution for the 5.48-MeV level has the basic  $l_n=2$  shape, it also appears to contain contributions from unresolved levels corresponding to different  $l_n$  values. The angular distribution for the 6.15-MeV level is very similar to that for the 5.13-MeV level and is given the tentative assignment  $J^\pi = (\frac{5}{2})^+$ .

Figure 25 shows the angular distributions from  $^{39}\text{Ca}$  levels at 2.47, 2.80, and 3.03 MeV. The 2.47-MeV level corresponds to  $l_n=0$  and thus has  $J^\pi = \frac{1}{2}^+$ . The shape of the distribution for the 2.80-MeV level is very similar to that for the transition to the 3.19-MeV level in  $^{35}\text{Ar}$ , which corresponds to an  $l_n=3$  pickup. Therefore, configuration mixing with the  $f_{7/2}$  shell is apparent in the  $^{40}\text{Ca}$  ground state, in qualitative agreement with the results of Ref. 29.

The 3.03-MeV level has been variously quoted as corresponding to an  $l_n=1$  and 2 neutron pickup in  $^{40}\text{Ca}(^3\text{He}, \alpha)^{39}\text{Ca}$  reactions,<sup>31,32</sup> while the mirror level appears to be excited by an  $l_p=1$  proton pickup in the  $^{40}\text{Ca}(d, ^3\text{He})^{39}\text{K}$  reaction.<sup>33</sup> The present result favors an  $l_n=1$  pickup with  $J^\pi = (\frac{1}{2}, \frac{3}{2})^-$ , in agreement with Refs.

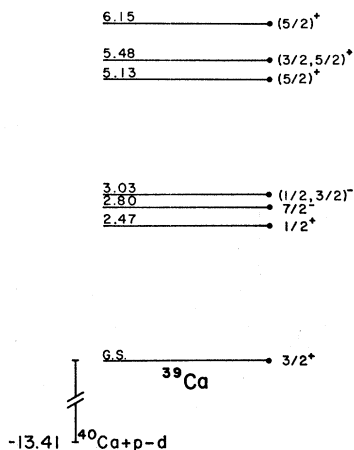


FIG. 26.  $^{39}\text{Ca}$  levels observed in the  $^{40}\text{Ca}(p, d)^{39}\text{Ca}$  reaction.

<sup>30</sup> P. E. Cavanagh, C. F. Coleman, G. A. Gard, B. W. Ridley, and J. F. Turner, Nucl. Phys. **50**, 49 (1964).

<sup>31</sup> D. Cline, W. Parker Alford, and L. M. Blau, Nucl. Phys. **73**, 33 (1965).

<sup>32</sup> R. Bock, H. H. Duhm, and R. Stock, Phys. Letters **18**, 61 (1965).

<sup>33</sup> J. C. Hiebert, E. Newman, and R. H. Bassel, Phys. Rev. **154**, 898 (1967).

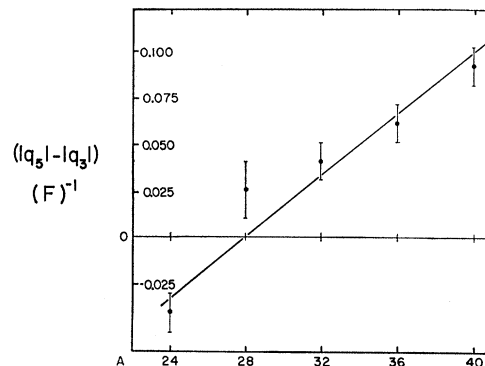


FIG. 27. Summary of experimental results for forward-angle  $J$  dependence.  $|q_5|$  ( $|q_3|$ ) is the momentum transferred to the residual nucleus for the forward maximum of the strongly excited  $\frac{5}{2}^+$  ( $\frac{3}{2}^+$ ) distribution of lowest energy.  $|q_5| - |q_3|$  is plotted versus mass number and a straight line is drawn for comparison. Estimates of the errors in determining the positions of the forward maxima are also shown.

31 and 33. Even though the statistics are poor, the angular distribution seems to be peaked at  $\theta_{\text{e.m.}} \approx 15^\circ$ , while the forward maxima of the  $l_n=2$  distributions are peaked at  $20^\circ$  to  $25^\circ$  at this bombarding energy. These results indicate that there is some configuration mixing with the  $2p$  shell as well as the  $f_{7/2}$  shell in the  $^{40}\text{Ca}$  ground state. The strengths of these admixtures are given in Sec. IV of this paper.

A summary of the excitation energies, spins, and parities of the  $^{39}\text{Ca}$  levels observed in the  $^{40}\text{Ca}(p, d)^{39}\text{Ca}$  reaction is shown in Fig. 26. The energy measurements are in agreement with those of Refs. 29 and 20, with an experimental error of about  $\pm 20$  keV. The  $J$  dependence in the angular distributions for the  $0.00(\frac{3}{2}^+)$ ,  $5.13(\frac{5}{2}^+)$ , and  $6.15\text{-MeV}(\frac{5}{2}^+)$  levels in  $^{39}\text{Ca}$  (Fig. 24) is very

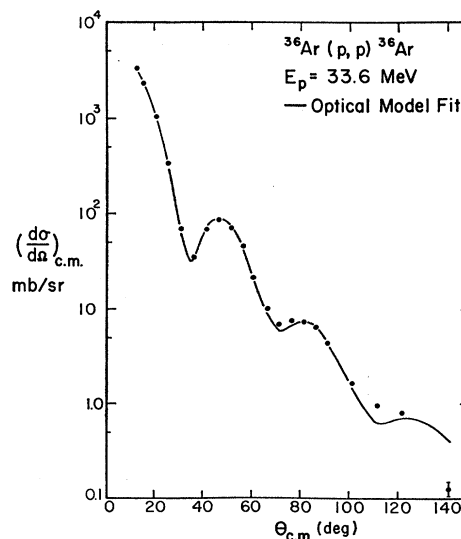


FIG. 28. Optical-model fit to the  $^{36}\text{Ar}(p, p)^{36}\text{Ar}$  elastic scattering data. The parameters are listed in Table I.

TABLE I. Optical-model parameters for DWBA analysis.

	$V_0$ (MeV)	$W$ (MeV)	$r_0$ (F)	$r_I$ (F)	$r_e$ (F)	$a_0$ (F)	$a_I$ (F)	Target A	Source
Protons	49.8	6.50	1.16	1.16	1.16	0.64	0.64	24, 28	$^{26}\text{Mg}(p,p)$
	47.1	6.87	1.18	1.18	1.18	0.66	0.66	32, 36, 40	$^{36}\text{Ar}(p,p)$
Deuterons	90.0	25.0 <sup>a</sup>	1.25	1.30	1.30	0.62	0.58	24-40	$^{36}\text{Ar}(p,p)$ b

<sup>a</sup> For the  $^{24}\text{Mg}(p,d)^{23}\text{Mg}$  reaction, an imaginary deuteron well depth of 35 MeV was used.  
<sup>b</sup> Reference 38.

similar to that observed in the  $^{36}\text{Ar}(p,d)^{35}\text{Ar}$  and  $^{32}\text{S}(p,d)^{31}\text{S}$  reactions.

### F. Summary of $J$ -Dependence Results

The  $J$  dependence observed in the forward angles of the  $l_n=2$  angular distributions seems to follow a systematic trend through the  $2s-1d$  shell. The forward maxima of the  $\frac{3}{2}^+$  angular distributions occur at smaller angles than the forward maxima of the  $\frac{5}{2}^+$  distributions for  $(p,d)$  reactions on  $^{40}\text{Ca}$ ,  $^{36}\text{Ar}$ , and  $^{32}\text{S}$ . The opposite effect is observed in the  $^{24}\text{Mg}(p,d)^{23}\text{Mg}$  reaction, while almost no effect is seen in the  $^{28}\text{Si}(p,d)^{27}\text{Si}$  reaction. Since there is evidence that the quadrupole deformation changes sign in the mass region  $A=28-30$ ,<sup>34</sup> it appears there may be some correlation between  $J$  dependence and the nature of the nuclear deformation. The effects for  $A>28$  are similar to those observed in the  $(p,d)$  reaction in the  $1f$  shell.<sup>4-6</sup> The  $J$  dependence at large angles appears to follow no definite pattern. For  $\theta_{c.m.} \lesssim 90^\circ$ , all of the  $\frac{5}{2}^+$  distributions are very similar in shape, while the  $\frac{3}{2}^+$  distributions sometimes undergo very distinct changes from nucleus to nucleus. The usefulness of  $J$  dependence as a spectroscopic tool has

been demonstrated by the assignment of spins to levels in  $^{31}\text{S}$ ,  $^{35}\text{Ar}$ , and  $^{39}\text{Ca}$ .

The experimental results for  $J$  dependence have been summarized by plotting the difference in positions of the forward maxima of  $\frac{3}{2}^+$  and  $\frac{5}{2}^+$  distributions versus mass number (Fig. 27). The vertical axis is in terms of the momentum transferred to the residual nucleus, which reduces the phase differences that may arise from the two levels of a given pair having different reaction  $Q$  values. The  $\frac{3}{2}^+$  and  $\frac{5}{2}^+$  distributions represented correspond to the strongly excited level of each respective spin having the lowest excitation energy. A DWBA analysis of  $J$  dependence and the extraction of spectroscopic factors to provide quantitative information on configuration mixing is presented in the next section.

## IV. ANALYSIS WITH THE DWBA AND COMPARISON TO THEORY

The experimental  $(p,d)$  angular distributions discussed in Sec. III were analyzed in the DWBA with respect to  $J$  dependence and the calculation of spectroscopic factors. The calculations were performed with the Macefield computer code in the zero-range approximation.

### A. Optical-Model Parameters

The optical-model parameters used to generate the incident-channel wave functions for the DWBA calcu-

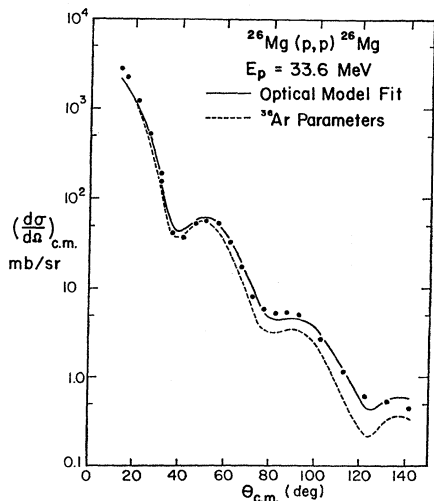


FIG. 29. Optical-model fits to the  $^{26}\text{Mg}(p,p)^{26}\text{Mg}$  elastic scattering data with  $^{36}\text{Ar}$  and  $^{26}\text{Mg}$  parameters. The parameters are listed in Table I.

<sup>34</sup> G. M. Crawley and G. T. Garvey, Phys. Rev. **160**, 981 (1967), and references therein.

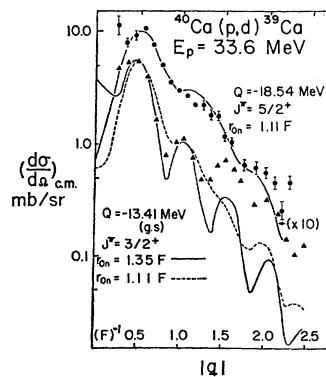


FIG. 30. DWBA fits to the  $l_n=2$   $J$ -dependence for the 5.13- ( $\frac{3}{2}^+$ ) and 0.00-MeV ( $\frac{3}{2}^+$ ) levels of  $^{39}\text{Ca}$  excited in the  $^{40}\text{Ca}(p,d)^{39}\text{Ca}$  reaction. The fit to the  $\frac{3}{2}^+$  distribution with the parameters for the  $\frac{5}{2}^+$  calculation is shown by the dashed curve. The forward maxima occur at  $\theta_{c.m.}=20^\circ-25^\circ$ , while a momentum transfer of  $1.5 \text{ F}^{-1}$  corresponds to a center-of-mass angle of approximately  $70^\circ$ .

lations were obtained from  $^{26}\text{Mg}(p, p)^{26}\text{Mg}$  and  $^{36}\text{Ar}(p, p)^{36}\text{Ar}$  elastic scattering experiments at 33.6-MeV bombarding energy. A best fit to the angular distributions was obtained by varying the parameters in an optical potential of Woods-Saxon form with surface absorption. The optical-model search program ABACUS<sup>35</sup> was used to obtain the fits to the data shown in Figs. 28 and 29. No spin-orbit interaction was included, since the DWBA code was not equipped to perform a spin-orbit calculation. The fit to the  $^{26}\text{Mg}$  data with the  $^{36}\text{Ar}$  parameters and the fit obtained in the search on  $^{26}\text{Mg}$  are shown in Fig. 29. As can be seen from Table I, the parameters are very similar for the two nuclei. It was therefore assumed that the basic optical parameters are reasonably constant with mass number in the  $2s-1d$  shell, and the  $^{26}\text{Mg}$  parameters were used in the DWBA calculations for the  $(p, d)$  reaction on  $^{24}\text{Mg}$  and  $^{28}\text{Si}$  while the  $^{36}\text{Ar}$  parameters were used for  $^{32}\text{S}$ ,  $^{36}\text{Ar}$ , and  $^{40}\text{Ca}$ .

Deuteron optical parameters have been obtained by Perey and Perey<sup>36,37</sup> for Ca and Mg nuclei at various bombarding energies, and by Cowley *et al.*<sup>38</sup> for  $^{27}\text{Al}$  and  $^{32}\text{S}$  targets at 15.8-MeV bombarding energy. An attempt to fit a  $(p, d)$  angular distribution was made with each set of parameters, but only those obtained in Ref. 38 for  $^{32}\text{S}$  resulted in reasonable DWBA fits to the data. These parameters are also listed in Table I and were used for all the targets in this work. An imaginary surface well depth ( $W$ ) of 25 MeV resulted in slightly better fits than the depth of 20 MeV obtained from the elastic scattering. It was necessary to further increase

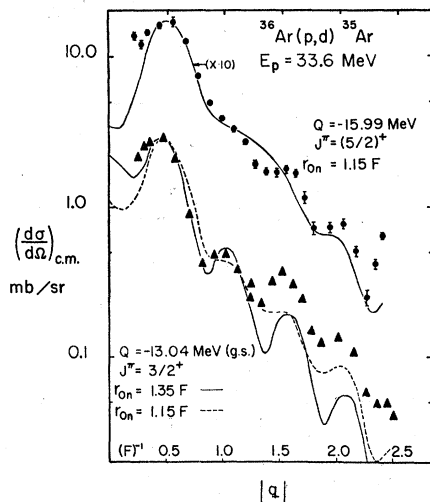


FIG. 31. DWBA fits to the  $l_n=2$   $J$ -dependence for the 2.95- ( $\frac{5}{2}^+$ ) and 0.00-MeV ( $\frac{3}{2}^+$ ) levels of  $^{35}\text{Ar}$  excited in the  $^{36}\text{Ar}(p, d)^{35}\text{Ar}$  reaction.

<sup>35</sup> E. H. Auerbach, Brookhaven National Laboratory Report No. 6562, 1962 (unpublished).

<sup>36</sup> C. M. Perey and F. G. Perey, Phys. Rev. **132**, 755 (1963).

<sup>37</sup> C. M. Perey and F. G. Perey, Oak Ridge National Laboratory Report No. ORNL-TM-1529, 1966 (unpublished).

<sup>38</sup> A. A. Cowley, G. Heymann, and R. L. Keizer, Nucl. Phys. **86**, 363 (1966).

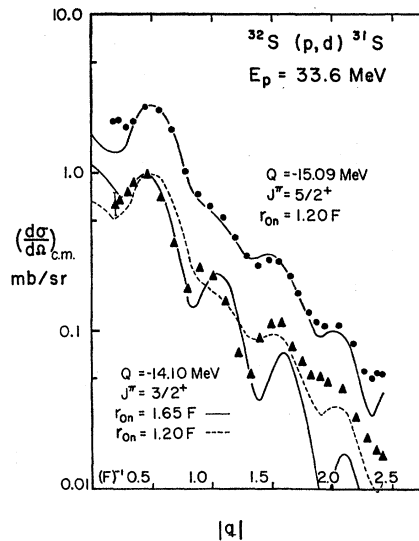


FIG. 32. DWBA fits to the  $l_n=2$   $J$ -dependence for the 2.23- ( $\frac{5}{2}^+$ ) and 1.24-MeV ( $\frac{3}{2}^+$ ) levels of  $^{31}\text{S}$  excited in the  $^{32}\text{S}(p, d)^{31}\text{S}$  reaction.

this depth to 35 MeV in order to obtain reasonable fits to the data from the  $^{24}\text{Mg}(p, d)^{23}\text{Mg}$  reaction.

### B. DWBA Analysis of $J$ Dependence

There have been two main approaches to the DWBA analysis of  $J$  dependence in the  $(p, d)$  reaction with regard to the bound-state form factor of the picked-up neutron. One is to assume different binding energies for neutrons that have different spins, even though their actual separation energies may be nearly the same. Both Sherr *et al.*<sup>4</sup> and Glashauser<sup>5</sup> have obtained satisfactory DWBA fits to the  $l_n=3$   $J$ -dependence using

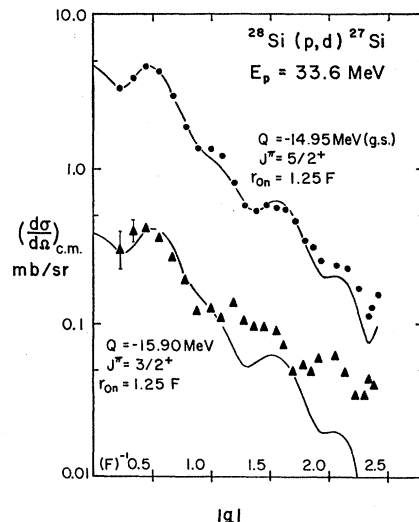


FIG. 33. DWBA fits to the 0.00- ( $\frac{5}{2}^+$ ) and 0.95-MeV ( $\frac{3}{2}^+$ ) levels of  $^{27}\text{Si}$  excited in the  $^{28}\text{Si}(p, d)^{27}\text{Si}$  reaction. Since little  $J$  dependence is observed in the forward angles, the same parameters are used in both calculations.

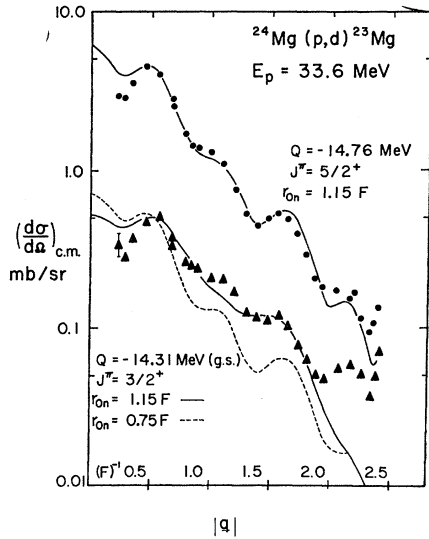


FIG. 34. DWBA fits to the  $l_n=2$   $J$ -dependence for the 0.45- ( $\frac{5}{2}^+$ ) and 0.00-MeV ( $\frac{3}{2}^+$ ) levels of  $^{23}\text{Mg}$  excited in the  $^{24}\text{Mg}(p,d)$ - $^{23}\text{Mg}$  reaction.

this method. However, this approach gives an incorrect asymptotic form for the neutron wave function. It has therefore been suggested<sup>39</sup> that other changes in the neutron well (e.g., radius or diffuseness) be employed, while maintaining the correct separation energy. An attempt to fit the  $l_n=3$   $J$ -dependence in the  $^{56}\text{Fe}(p,d)$ - $^{55}\text{Fe}$  reaction by changing the neutron well radius has been made by Glashauser<sup>5</sup> and was partially successful at his highest bombarding energy (27.5 MeV). The same method has been used to fit the  $l_n=2$   $J$ -dependence at the forward angles in the present work.

The Woods-Saxon potential

$$V(r) = -V_0 \{1 + \exp[(r - r_{0n}A^{1/3})/a_n]\}^{-1}$$

was used for the bound neutron, where the depth  $V_0$  is determined by the neutron binding energy. The radius corresponding to the pickup of a  $d_{5/2}$  neutron was kept constant at  $3.79 \text{ F} = 1.25(28)^{1/3} \text{ F}$  for all targets having  $A \geq 28$ . This effectively assumes a  $^{28}\text{Si}$  core that does not change in physical size. The radius parameter  $r_{0n}$  was then varied in an attempt to obtain a fit to the positions and shape of the forward maximum in a  $J^\pi = \frac{3}{2}^+$  angular distribution for each nucleus. The diffuseness  $a_n$  was kept constant at 0.65 F for all cases shown here, except for the fit to the  $\frac{3}{2}^+$  distribution in  $^{31}\text{S}$  (see below).

A pair of levels from each nucleus, one having  $J^\pi = \frac{3}{2}^+$  and one  $\frac{5}{2}^+$ , was selected for this analysis. The strongly excited level corresponding to the lowest excitation energy was chosen for each spin, and the differential cross sections of these levels are plotted in Figs. 30-34 versus  $|\mathbf{q}|$ , the momentum transferred to the residual nucleus. The  $\frac{5}{2}^+$  distributions always appear at the top of the figure, and are renormalized as indicated. A

<sup>39</sup> W. T. Pinkston and G. R. Satchler, Nucl. Phys. **72**, 641 (1965).

TABLE II. Summary of neutron parameters for DWBA analysis of  $J$  dependence.

Target	$a_{0n}$ (F)	$R_{3/2}$ (F)	$R_{5/2}$ (F)	$R_{3/2}/R_{5/2}$	$\frac{\sigma(R_{3/2})/\sigma(R_{5/2})^a}{\sigma(R_{5/2})^a}$
$^{24}\text{Mg}$	0.65	2.16	3.32	0.65	0.5
$^{28}\text{Si}$	0.65	3.79	3.79	1.00	1.0
$^{32}\text{S}$	0.65	5.55	3.79	1.46	5.0
		0.75	5.23	(3.79)	(1.37)
$^{36}\text{Ar}$	0.65	4.46	3.79	1.17	1.7
$^{40}\text{Ca}$	0.65	4.62	3.79	1.22	1.9

<sup>a</sup> Ratio of DWBA cross sections at forward maxima.

momentum transfer of  $1.5 \text{ F}^{-1}$  corresponds to a center-of-mass angle of approximately  $70^\circ$ .

### 1. $^{40}\text{Ca}(p,d)^{39}\text{Ca}$

Figure 30 shows DWBA fits to the distributions for the ground ( $\frac{3}{2}^+$ ) and 5.13-MeV ( $\frac{5}{2}^+$ ) levels of  $^{39}\text{Ca}$ . The neutron well radius parameter of 1.11 F for the  $J^\pi = \frac{5}{2}^+$  calculations arises from the assumption of a constant  $d_{5/2}$  radius ( $R_{5/2} = 3.79 \text{ F}$ ), and seems to give a reasonable fit to the data. As is shown by the dashed curve, this same radius does not result in a good fit to the forward maximum of the ground-state ( $\frac{3}{2}^+$ ) distribution. A larger radius ( $r_{0n} = 1.35 \text{ F}$ ) predicts the oscillatory structure of the  $J^\pi = \frac{3}{2}^+$  distribution more accurately for  $|\mathbf{q}| \lesssim 1.2 \text{ F}^{-1}$ , but it predicts too small a cross section for higher momentum transfers.

### 2. $^{36}\text{Ar}(p,d)^{35}\text{Ar}$

The  $J$  dependence observed in the distributions for the ground ( $\frac{3}{2}^+$ ) and 2.95-MeV ( $\frac{5}{2}^+$ ) levels of  $^{35}\text{Ar}$  (Fig. 31) is very similar to that from the  $^{40}\text{Ca}(p,d)^{39}\text{Ca}$  reaction, and similar neutron parameters were used in the DWBA calculation with about the same degree of success. The assumed  $d_{5/2}$  radius of 3.79 F corresponds to an  $r_{0n}$  of 1.15 F, while the  $r_{0n}$  for  $J^\pi = \frac{3}{2}^+$  (1.35 F) is the same as that used to fit the  $^{39}\text{Ca}$  ground-state distribution.

### 3. $^{32}\text{S}(p,d)^{31}\text{S}$

As was described earlier (Sec. III), the  $J$  dependence for the 2.23-MeV ( $\frac{5}{2}^+$ ) and 1.24-MeV ( $\frac{3}{2}^+$ ) levels of  $^{31}\text{S}$  is very pronounced. The DWBA fits to the data for these levels are shown in Fig. 32, where it is seen that the fit to the  $J^\pi = \frac{5}{2}^+$  distribution is quite good. The  $\frac{3}{2}^+$  distribution drops much more rapidly from the forward maximum than the  $\frac{5}{2}^+$  data, and this is not reproduced by using the assumed  $d_{5/2}$  neutron well radius ( $r_{0n} = 1.20 \text{ F}$ ) in the DWBA calculation. The radius parameter was increased to 1.65 F and the diffuseness to 0.75 F in order to fit the data for  $|\mathbf{q}| \gtrsim 0.8 \text{ F}^{-1}$ ; however, this resulted in a wrong prediction for the position of the second maximum at  $|\mathbf{q}| \sim 0.9 \text{ F}^{-1}$ . A calculation where  $r_{0n} = 1.75 \text{ F}$  and  $a_n = 0.65 \text{ F}$  (not shown) fits the forward angles equally well but results in an even worse prediction for the second maximum.

TABLE III. Spectroscopic factors for the  $^{24}\text{Mg}(p,d)^{23}\text{Mg}$  reaction.

$E_x$ (MeV)	$\sigma_{\text{max}}$ (mb/sr)	$J^\pi$	$S_{\text{expt}}(r_{0n}=1.15 \text{ F})$	Theory <sup>a</sup>	
				$J^\pi$	$S_T$
0.00	0.52	$\frac{3}{2}^+$	0.72		
0.45	4.5	$\frac{5}{2}^+$	5.66	$\frac{5}{2}^+$	3.22
2.35	0.31 (30°)	$\frac{1}{2}^+$	0.20	$\frac{1}{2}^+$	0.37
2.71	2.65	$(\frac{3}{2}, \frac{3}{2})^-$	3.40 <sup>b</sup>		
			0.80 <sup>c</sup>		
3.79	1.0	$(\frac{1}{2}, \frac{3}{2})^-$	1.69 <sup>b</sup>		
			0.38 <sup>c</sup>		
4.37	0.09 (30°)	$\frac{1}{2}^+$	0.10	$\frac{1}{2}^+$	0.007
5.32	0.31	$(\frac{3}{2}, \frac{3}{2})^+$	0.54		
6.02	0.62	$(\frac{1}{2}, \frac{3}{2})^-$	2.04 <sup>b</sup>		
			0.44 <sup>c</sup>		
9.63	0.17	$(\frac{3}{2}^+, \frac{5}{2}^+)$	1.05		

<sup>a</sup> Predictions of Ref. 42.

<sup>b</sup> Assuming pickup from 1p shell.

<sup>c</sup> Assuming pickup from 2p shell.

#### 4. $^{28}\text{Si}(p,d)^{27}\text{Si}$

The distributions for the ground ( $\frac{5}{2}^+$ ) and 0.95-MeV ( $\frac{3}{2}^+$ ) levels of  $^{27}\text{Si}$  are shown in Fig. 33, where little  $J$  dependence is observed. The position of the forward maximum of the  $\frac{3}{2}^+$  distribution appears to occur at a slightly smaller  $|\mathbf{q}|$  than the  $\frac{5}{2}^+$  maximum. However, the slope following the maximum is, if anything, *less* steep for  $J=\frac{3}{2}$  than for  $J=\frac{5}{2}$ . These two effects compete when the neutron radius or diffuseness is varied in the distorted-wave calculation, so no variations were made in this case. The DWBA prediction is shown normalized to the data for both levels and is in good agreement with the shape of the ground-state ( $\frac{5}{2}^+$ ) distribution.

#### 5. $^{24}\text{Mg}(p,d)^{23}\text{Mg}$

The experimentally observed  $J$ -dependence effects in the distributions for the ground ( $\frac{3}{2}^+$ ) and 0.45-MeV ( $\frac{5}{2}^+$ ) levels of  $^{23}\text{Mg}$  are generally opposite to those observed in the  $(p,d)$  reaction on the other nuclei studied. The DWBA calculations for these distributions were made with an imaginary deuteron well depth of 35 MeV and are shown in Fig. 34. A depth of 25 MeV, which was used for all of the other nuclei, resulted in a curve having much less structure and no relative minimum for small  $|\mathbf{q}|$ . Also, the  $d_{5/2}$  radius used here is  $1.15(24)^{1/3} \text{ F} = 3.32 \text{ F}$  instead of the 3.79 F used for all the other nuclei. It is seen that the value for  $r_{0n}$  of 1.15 F is too large to yield an acceptable DWBA fit to the  $\frac{3}{2}^+$  distribution. This was decreased to 0.75 F to obtain a reasonable approximation to the forward maximum and overall slope of the data.

#### 6. Summary of $J$ -Dependence Analysis

The use of different radii in the neutron form factor for  $d_{3/2}$  and  $d_{5/2}$  pickups was at least partially successful in predicting the  $l_n=2$   $J$ -dependence at the forward angles. It must be emphasized, however, that this analysis serves only to illustrate the extent to which the radius must be changed. The results are summarized in

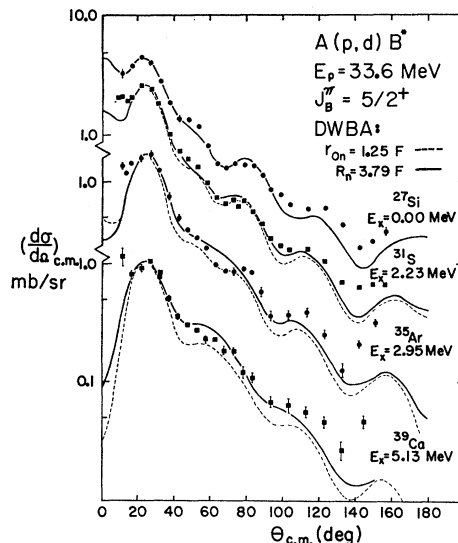


FIG. 35. DWBA fits to the  $\frac{5}{2}^+$  angular distributions for levels excited in the  $(p,d)$  reaction on  $^{28}\text{Si}$ ,  $^{32}\text{S}$ ,  $^{36}\text{Ar}$ , and  $^{40}\text{Ca}$ . The DWBA predictions for a constant total neutron-well radius (3.79 F) and a constant well-radius parameter (1.25 F) are represented by solid and dashed curves, respectively.

Table II, where  $R_{3/2}$  and  $R_{5/2}$  correspond to  $r_{0n}A^{1/3}$  for  $d_{3/2}$  and  $d_{5/2}$  pickups, respectively. The radial change is quite large for most of the targets studied and, as can be seen from the ratio  $\sigma(R_{3/2})/\sigma(R_{5/2})$  in Table II, a large change in radius results in a large change in the magnitude of the calculated DWBA cross section. This gives rise to problems in extracting absolute spectroscopic factors, as will be seen in Sec. IV C. It is interesting to note, however, that the ratio of the  $d_{3/2}$  radius to the  $d_{5/2}$  radius ( $R_{3/2}/R_{5/2}$ ) is, in general, closer to unity than the ratio of the semiaxes of the nuclear ellipsoid if one assumes reasonable values for the deformation parameter.<sup>40,41</sup> The only exception to this is the case of  $^{40}\text{Ca}$ .

The effect of using a constant radius for a  $d_{5/2}$  neutron is summarized in Fig. 35, which shows a comparison of the DWBA fits to the  $\frac{5}{2}^+$  angular distributions for  $R_{5/2}=3.79 \text{ F}$  and  $1.25 A^{1/3} \text{ F}$ . The fits to the distributions for all the levels are reasonable at forward angles with the smaller radius (3.79 F), while the predictions for a radius of  $1.25 A^{1/3} \text{ F}$  are in less agreement with the data as  $A$  increases. The effect is not large, however, and the quality of the DWBA fits for  $R_{5/2}=3.79 \text{ F}$  is not the same for the distributions of all the nuclei at large angles.

#### C. DWBA Spectroscopic Factors

The  $(p,d)$  spectroscopic factors were calculated using the optical-model parameters mentioned earlier, and are presented for each nucleus in Tables III–VII. The

<sup>40</sup> P. H. Stelson and Lee Grodzins, Nucl. Data A1, 21 (1965).

<sup>41</sup> J. L. Snelgrove and E. Kashy, Bull. Am. Phys. Soc. 12, 681 (1967).

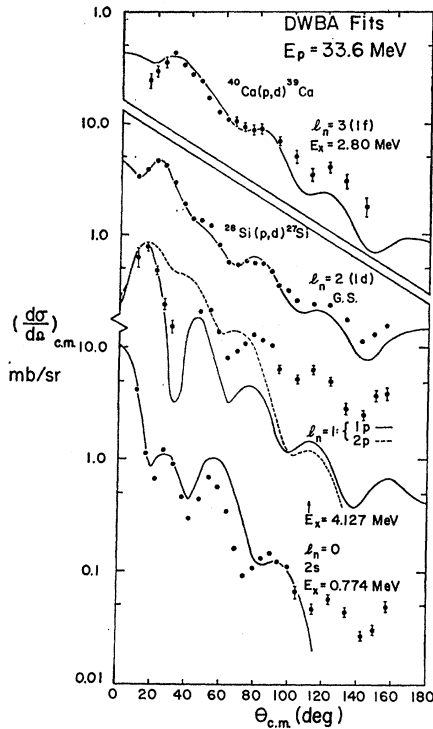


FIG. 36. DWBA calculations for different values of  $l_n$ . Fits for the 2.80-MeV level of  $^{39}\text{Ca}$  ( $l_n=3$ ) and for the 0.00- ( $l_n=2$ ), 4.127- ( $l_n=1$ ), and 0.774-MeV ( $l_n=0$ ) levels of  $^{27}\text{Si}$  are shown.

neutron parameters were chosen from those used for the  $J$ -dependence analysis (Table II), and DWBA results for both neutron well radii are present for some of the levels in  $^{31}\text{S}$ ,  $^{35}\text{Ar}$ , and  $^{39}\text{Ca}$ . Although the DWBA calculations resulted in quite satisfactory fits to the  $l_n=2$  data (especially the  $\frac{5}{2}^+$  distributions), the predictions for the other  $l_n$  values were not as good. Figure 36 shows DWBA fits to the data corresponding to  $1d$ ,  $2s$ ,  $1p$ , and  $2p$  neutron transfers in the  $^{28}\text{Si}(p,d)^{27}\text{Si}$  reaction and the fit to the  $l_n=3$  distribution in the  $^{40}\text{Ca}(p,d)^{39}\text{Ca}$  reaction.

TABLE IV. Spectroscopic factors for the  $^{28}\text{Si}(p,d)^{27}\text{Si}$  reaction.

$E_x$ (MeV)	$\sigma_{\max}$ (mb/sr)	$J^\pi$	$S_{\text{expt}}(r_{0n}=1.25 F)$
0.00	4.6	$\frac{5}{2}^+$	3.45
0.774	1.2(28°)	$\frac{3}{2}^+$	0.64
0.952	0.41	$\frac{3}{2}^+$	0.34
2.647	0.5	$\frac{5}{2}^+$	0.47
2.90 <sup>a</sup>	0.84	$(\frac{3}{2}, \frac{5}{2})^+$	(0.81)
4.127	0.80	$(\frac{1}{2}, \frac{3}{2})^-$	1.20 <sup>b</sup>
			0.21 <sup>c</sup>
4.275	0.3	$(\frac{3}{2}, \frac{5}{2})^+$	0.34
5.233	0.84	$(\frac{1}{2}, \frac{3}{2})^-$	1.67 <sup>b</sup>
			0.28 <sup>c</sup>
6.343	0.30	$(\frac{3}{2}, \frac{5}{2})^+$	0.45

<sup>a</sup> Unresolved doublet.

<sup>b</sup> Assuming pickup from  $1p$  shell.

<sup>c</sup> Assuming pickup from  $2p$  shell.

TABLE V. Spectroscopic factors for the  $^{32}\text{S}(p,d)^{31}\text{S}$  reaction.

$E_x$ (MeV)	$\sigma_{\max}$ (mb/sr)	$J^\pi$	$S_{\text{expt}}(r_{0n}=1.20 F)$
0.00	3.6(27°)	$\frac{1}{2}^+$	1.04
1.24	1.0	$\frac{3}{2}^+$	0.94
			0.18 <sup>a</sup>
2.23	2.7	$\frac{5}{2}^+$	2.77
3.29	0.6	$(\frac{3}{2}, \frac{5}{2})^+$	0.73
4.09	0.7	$\frac{5}{2}^+$	0.86
4.72	0.4(27°)	$(\frac{1}{2}, \frac{3}{2})^+$	0.07
7.05	0.6	$(\frac{3}{2}, \frac{5}{2})^+$	1.00

<sup>a</sup>  $r_{0n}=1.65 F$ ,  $a_n=0.75 F$ .

The experimental spectroscopic factors for levels excited in the  $^{24}\text{Mg}(p,d)^{23}\text{Mg}$  reaction are listed in Table III along with the results of shell-model calculations by Wildenthal.<sup>42</sup> An unusually deep imaginary well (35 MeV) was required in the deuteron channel in order to obtain reasonable DWBA fits to the data. This caused a decrease in magnitude of the calculated  $l_n=2$  cross sections, which resulted in values for the spectroscopic factors that are unreasonably large if one assumes  $^{24}\text{Mg}$  has a closed  $^{16}\text{O}$  core. The values in Table III are therefore to be trusted only on a relative basis. Nevertheless, the ratio of the experimental spectroscopic factors ( $S_{\text{expt}}$ ) for the  $\frac{1}{2}^+$  levels at 2.35 and 4.37 MeV is in poor agreement with the ratio obtained from Wildenthal's calculations for levels at 1.80 and 4.81 MeV.

The experimental spectroscopic factors were compared to those predicted by the Nilsson-model wave functions of Chi.<sup>43</sup> However, since each Nilsson orbit can hold only two neutrons, the spectroscopic factors for the low-lying levels in  $^{27}\text{Si}$ ,  $^{31}\text{S}$ , and  $^{35}\text{Ar}$  (Tables IV–VI) are too large to correspond to pure rotational bands. As can be seen from the spectroscopic factors listed in Table IV, approximately half of the  $2s$ - $1d$  shell strength is contained in the ground-state ( $d_{5/2}$ ) transition for the  $^{28}\text{Si}(p,d)^{27}\text{Si}$  reaction. The value of 3.45 for  $S_{\text{expt}}$  agrees reasonably well with values of 3.9 and 3.97 obtained from  $^{28}\text{Si}(d,^3\text{He})^{27}\text{Al}$  proton pickup reactions.<sup>21,22</sup>

TABLE VI. Spectroscopic factors for the  $^{36}\text{Ar}(p,d)^{35}\text{Ar}$  reaction.

$E_x$ (MeV)	$\sigma_{\max}$ (mb/sr)	$J^\pi$	$r_{0n}=1.15 F$	$S_{\text{expt}} r_{0n}=1.35 F$
0.00	2.9	$\frac{3}{2}^+$	3.03	1.76 <sup>a</sup>
1.18	3.4(26°)	$\frac{1}{2}^+$	1.29	1.05
1.70	...	$(\frac{5}{2}, \frac{3}{2})^+$	0.1	
2.60	0.3	$(\frac{3}{2}, \frac{5}{2})^+$	0.42	0.28 <sup>a</sup>
2.95	1.7	$(\frac{5}{2}, \frac{3}{2})^+$	2.31 <sup>a</sup>	1.53
3.19	0.3	$\frac{7}{2}^-$	0.64	0.37 <sup>a</sup>
4.70	0.07(26°)	$(\frac{1}{2}, \frac{3}{2})^-$	0.05	0.04
5.57	1.0	$(\frac{3}{2}, \frac{5}{2})^+$	1.77 <sup>a</sup>	1.25
6.01	0.6	$(\frac{5}{2}, \frac{3}{2})^+$	1.18	0.83 <sup>a</sup>
6.62	0.3(24°)	$(\frac{1}{2}, \frac{3}{2})^-$	0.24	0.19
6.82	0.4	$(\frac{3}{2}, \frac{5}{2})^+$	0.72 <sup>a</sup>	0.51

<sup>a</sup> Value for radius giving best DWBA fit.

<sup>42</sup> B. H. Wildenthal (private communication).

<sup>43</sup> B. E. Chi, Nucl. Phys. 83, 97 (1966).

TABLE VII. Spectroscopic factors for the  $^{40}\text{Ca}(p, d)^{39}\text{Ca}$  reaction.

$E_x$ (MeV)	$\sigma_{\text{max}}$ (mb/sr)	$J^\pi$	$S_{\text{expt}}$	
			$r_{0n} = 1.11 \text{ F}$	$r_{0n} = 1.35 \text{ F}$
0.00	5.6	$\frac{3}{2}^+$	7.11	3.70 <sup>a</sup>
2.47	3.0(26°)	$\frac{1}{2}^+$	2.31	1.82
2.80	0.4	$\frac{1}{2}^-$	1.04	0.58 <sup>a</sup>
3.03	0.2	$(\frac{3}{2}, \frac{3}{2})^-$		0.02
5.13	1.1	$(\frac{5}{2})^+$	2.08 <sup>a</sup>	1.43
5.48	0.5	$(\frac{3}{2}, \frac{5}{2})^+$	0.97	0.67
6.15	1.0	$(\frac{5}{2})^+$	2.15 <sup>a</sup>	1.48

<sup>a</sup> Values for radius giving best DWBA fit.

It has been suggested<sup>20</sup> that the  $^{27}\text{Al}$  mirror nucleus has a prolate deformation where the first few excited levels correspond to a rotational band based on the  $K = \frac{1}{2}$  [211] Nilsson orbit (Fig. 3). The excitation of the corresponding levels in  $^{27}\text{Si}$  by a direct-pickup process [such as the  $(p, d)$  reaction] would then indicate configuration mixing with Nilsson orbit 9 in the  $^{28}\text{Si}$  ground state. However, there seems to be no prolate value for  $\delta (> 0)$  for which the  $K = \frac{1}{2}$  [211] wave function of  $\text{Chi}^{43}$  is in reasonable relative agreement with the experimental values for the levels at 0.774( $\frac{1}{2}^+$ ), 0.952( $\frac{3}{2}^+$ ), and 2.647( $\frac{5}{2}^+$ ) MeV (Table IV). Since the  $\frac{5}{2}^+$  assignment for the  $^{27}\text{Si}$  ground state is inconsistent energywise with an oblate deformation (Fig. 3), it appears that no simple form of the strong-coupling model can explain the results. The large spectroscopic factor for the ground-state transition is some indication that the average deformation is probably small and that the mixing of rotational bands is extensive. It has been suggested that the  $^{28}\text{Si}$  nucleus undergoes shape oscillations, since the energy minima for the prolate and oblate solutions are nearly equal in a Hartree-Fock calculation.<sup>44</sup>

Spectroscopic factors for the  $l_n = 1$  levels excited in the  $(p, d)$  reaction on  $^{24}\text{Mg}$  and  $^{28}\text{Si}$  were calculated for both a  $1p$  and a  $2p$  origin for the transferred neutron. As can be seen from Tables III and IV, the values assuming a  $2p$  pickup are considerably smaller than those for a  $1p$  pickup.

DWBA spectroscopic factors were calculated for both neutron well radii used in the analysis for  $J$  dependence for the 1.24-MeV level in  $^{31}\text{S}$  (Table V) and for several levels in  $^{35}\text{Ar}$  and  $^{39}\text{Ca}$  (Tables VI and VII). These results illustrate the ambiguity involved in extracting spectroscopic factors when the  $J$  dependence is strong. The results from the  $^{32}\text{S}(p, d)^{31}\text{S}$  reaction (Table V) are in good agreement with the relative spectroscopic factors obtained from the  $^{32}\text{S}(^3\text{He}, \alpha)^{31}\text{S}$  reaction,<sup>45</sup> except that in the  $(^3\text{He}, \alpha)$  reaction the level at 4.45 MeV is also strongly excited. The  $S_{\text{expt}}$  value corresponding to the best DWBA fit for the  $l_n = 2$  and  $l_n = 3$  levels of  $^{35}\text{Ar}$  and  $^{39}\text{Ca}$  are denoted by a superscript  $a$  in Tables VI and VII and appear to be in good agreement with the total expected  $l_n = 2$  strength ( $\sim 8$  and  $10$ , respectively).

<sup>44</sup> R. Muthukrishnan, Nucl. Phys. A93, 417 (1967).

<sup>45</sup> C. M. Fou and R. W. Zurmühle, Phys. Rev. 151, 927 (1966).

The spectroscopic factor of 0.58 for the  $l_n = 3$  level at 2.80 MeV in  $^{39}\text{Ca}$  (Table VII) is in good agreement with the value of 0.53 obtained by Bock *et al.*<sup>32</sup> from the  $^{40}\text{Ca}(^3\text{He}, \alpha)^{39}\text{Ca}$  reaction and with the result of 0.5 obtained for the excitation of the mirror level in the  $^{40}\text{Ca}(d, ^3\text{He})^{39}\text{K}$  reaction.<sup>33</sup> Glashauser *et al.*<sup>29</sup> extracted values of 0.14 and 0.28 by assuming different neutron separation energies in the  $^{40}\text{Ca}(p, d)^{39}\text{Ca}$  reaction at 27.3-MeV bombarding energy. The excitation of the  $l_n = 1$  level at 3.03 MeV is assumed to be due to a  $2p$  shell admixture with an estimated spectroscopic factor of  $\sim 0.02$ , as compared to a value of 0.04–0.05 obtained by Hiebert *et al.*<sup>33</sup> for the mirror level in the  $(d, ^3\text{He})$  reaction mentioned above. Both of these results are considerably smaller than the value 0.11 obtained by Cline *et al.*<sup>31</sup> from the  $^{40}\text{Ca}(^3\text{He}, \alpha)^{39}\text{Ca}$  reaction. The spectroscopic factors for the  $l_n = 2$  levels at 5.13, 5.48, and 6.15 MeV in  $^{39}\text{Ca}$ , together with the lack of any strong excitation above 6.15 MeV, indicate that these levels represent most of the  $d_{5/2}$  strength.

## V. SUMMARY AND CONCLUSIONS

The investigation of the  $(p, d)$  reaction on  $N = Z$  nuclei in the  $2s-1d$  shell has provided new information about the level structures of the  $^{28}\text{Mg}$ ,  $^{27}\text{Si}$ ,  $^{31}\text{S}$ , and  $^{35}\text{Ar}$  residual nuclei, while previous results for  $^{39}\text{Ca}$  have been confirmed.<sup>29, 31</sup> The 33.6-MeV bombarding energy and particle-detection techniques have permitted the observation of 10–12 MeV of excitation in the residual nuclei, with the interesting result that virtually all of the observed  $2s-1d$  shell hole strength exists at excitation energies  $\lesssim 8$  MeV. (A possible exception to this is the 9.63-MeV level in  $^{28}\text{Mg}$ .) It is therefore apparent that most of the  $2s-1d$  shell hole states have been excited; the DWBA spectroscopic factors obtained here are in support of this fact.

The forward-angle  $J$  dependence observed in the  $l_n = 2$  angular distributions appears to vary in a systematic way with mass number (for  $N = Z$  targets) (Fig. 27), and seems to be correlated with the nature of the nuclear deformation. The attempts to reproduce  $J$ -dependence effects by varying the neutron well radius in distorted-wave calculations were partially successful. Large changes were necessary in most cases, however, which produced correspondingly large changes in the magnitude of the calculated DWBA cross section and led to uncertainties in extracting spectroscopic factors. However, there is some evidence that the radius parameter corresponding to the best DWBA fit to the data might also result in the most trustworthy value for the spectroscopic factor. It is apparent from the results of this and other investigations<sup>3–6</sup> that additional experimental information and more theoretical work is necessary to obtain an understanding of  $J$  dependence. Distorted-wave calculations which explicitly account for nuclear deformations may give further insight to this problem.

Of particular interest is the excitation of low-lying ( $E_x=2.7-6.0$  MeV)  $l_n=1$  levels in  $^{32}\text{Mg}$  and  $^{27}\text{Si}$ , which could be due to configuration mixing with the  $2p$  shell. However, a plot of  $(p,d)$  reaction  $Q$  values for the excitation of the first  $l_n=1$  level versus mass number (Fig. 12) seems to be strong evidence that these levels are  $1p$  shell hole states.

The ordering of the first few levels in  $^{28}\text{Mg}$ ,  $^{31}\text{S}$ , and  $^{38}\text{Ar}$  seems to be qualitatively consistent with rotational bands based on neutron holes in Nilsson orbits (Ref. 14 and Fig. 3). However, the extraction of DWBA spectroscopic factors has shown that the states are considerably

more complex. The large spectroscopic factors measured for the excitation of low-lying levels in  $^{31}\text{S}$ ,  $^{35}\text{Ar}$ , and especially  $^{27}\text{Si}$  are indications of considerable rotational band mixing.

#### ACKNOWLEDGMENTS

The author is greatly indebted to Professor E. Kashy for his advice and many helpful discussions concerning this work. He also wishes to thank Dr. L. A. Kull and P. J. Plauger for their help in taking the data, and Professor W. P. Johnson for his advice in the operation of the cyclotron.

### Excitation Functions for Radioactive Isotopes Produced by Proton-Induced Reactions in Silicon\*

D. W. SHEFFEY

*University of Tennessee, Knoxville, Tennessee*

AND

I. R. WILLIAMS†

*Knoxville College, Knoxville, Tennessee*

AND

C. B. FULMER

*Oak Ridge National Laboratory, Oak Ridge, Tennessee*

(Received 11 April 1968)

Cross sections were measured for the production of radioactive nuclides by proton-induced reactions in natural silicon at bombarding energies below 60 MeV. Stacked wafers of target material were bombarded with cyclotron-accelerated protons.  $\gamma$  spectra of individual foils were subsequently measured with a Ge(Li) spectrometer. Excitation functions were obtained for  $^{28}\text{Al}$ ,  $^{29}\text{Al}$ ,  $^{27}\text{Mg}$ ,  $^{22}\text{Na}$ ,  $^{24}\text{Na}$ ,  $^{18}\text{F}$ , and  $^7\text{Be}$ . Cross sections predicted by an evaporation theory are in reasonable agreement with the experimental values.

#### INTRODUCTION

EXCITATION functions for proton-induced reactions can yield information about reaction mechanisms, they can be used to estimate residual radiation levels in the vicinity of particle accelerators, and they contribute information about the interaction of primary cosmic rays (which are  $\sim 90\%$  protons) with matter. Although silicon has a relatively large cosmic abundance, only one measurement<sup>1</sup> of the excitation function for a proton-induced reaction in silicon has been reported for bombarding energies below 60 MeV.

The high-resolution Ge(Li)  $\gamma$  spectrometer<sup>2</sup> has made

the measurements of excitation functions for production of radioactive products relatively easy.

In the work reported here measurements were made of the excitation functions for the production of seven radionuclides in natural silicon by proton bombardment at energies below 60 MeV. The most ephemeral nuclide has a half-life of 2.3 min.

#### EXPERIMENTAL

Stacks of wafers of natural silicon were bombarded in a proton beam at the Oak Ridge Isochronous Cyclotron. The available wafers varied in thickness from 0.028 to 0.114 in. The proton beam was focused to a diameter of 0.25 in. at the target position. The target assembly served as a Faraday cup to monitor the beam intensity, which was uniform within 5% for the duration of each bombardment. Integrated beams of  $\sim 10^{13}$  protons were used for each bombardment. The un-

\* Research sponsored by the U. S. Atomic Energy Commission under contract with the Union Carbide Corporation. This paper is based on a thesis submitted by D. W. Sheffey to the Graduate Council of the University of Tennessee, December, 1967, in partial fulfillment of the requirements for the degree of Master of Science.

† Consultant to Oak Ridge National Laboratory.

<sup>1</sup> B. L. Cohen, Phys. Rev. **102**, 453 (1956).

<sup>2</sup> R. J. Fox, I. R. Williams, and K. S. Toth, Nucl. Instr. Methods **35**, 331 (1965); G. T. Ewan and A. J. Tavendale, Can. J. Phys.

**42**, 2286 (1964); W. L. Hansen and B. V. Jarrett, Nucl. Instr. Methods **31**, 301 (1964).